

Estimation of antigen-responsive T-cell frequencies in PBMC from human subjects

Karl Broman*, Terry Speed* and Michael Tigges†

Technical Report #454

March 26, 1996

Abstract

A new method for estimating the frequency of antigen-responsive T-cells, using a cell proliferation assay, is described. In this assay, the uptake of tritiated thymidine, by peripheral blood mononuclear cells which have been exposed to antigen, is measured for each well on a microtiter plate. Whereas this assay is generally used as part of a limiting dilution assay, here we estimate the frequency of responding cells using a single, carefully chosen cell density. The traditional analysis of such data uses a cut-off to separate wells which contain no responding cells and wells which contain at least one responding cell. The new method uses the scintillation count to estimate the number of responding cells for each well on the plate.

*Department of Statistics, University of California, Berkeley

†The Biocine Company, Chiron Corporation, Emeryville, California

1 Introduction

In this paper we describe a method for estimating the frequency of antigen-responsive T-cells among peripheral blood mononuclear cells (PBMC) from human subjects. It was developed in a particular context, but we believe that the approach may have wider applicability. The proliferation assay which motivates our method seeks to quantitate the response of human subjects to a herpes simplex vaccine consisting of HSV type 2 glycoproteins D and B, expressed as recombinant proteins in Chinese hamster ovary cells and administered as a vaccine combined with alum (Parr et al., 1991; Straus et al., 1993) or an oil-in-water emulsion adjuvant MF59 (Langenberg et al., 1995). A standard proliferation assay (James, 1991) utilizing the responses in triplicate wells was found to be inadequate in this context, while a full limiting dilution assay (LDA) was not feasible because of the need for more PBMC than were available from the vaccine recipients. Accordingly, our analysis was developed for estimating the number of antigen-responsive T-cells based on a single carefully chosen dilution, and so we sought to make greater use of the data than is usually the case.

Two other factors prompted our approach, which we now describe. In the present context, a standard LDA begins with a classification of the wells in all or part of a microtiter plate into the categories positive (contains at least one responding cell) and negative (contains no responding cells). Use is then made of a statistical model, typically the single-hit Poisson model (SHPM), which relates the frequency of positive wells to the frequency of responding cells in the wells. The frequency of responding cells is then estimated from the data on wells using the method of maximum likelihood or minimum chi-square. All

such analyses have to use some method of determining which wells contain responding cells, that is, of classifying wells into positives and negatives. The data with which this classification is done is generally a scintillation count, and it is usual for the assay to contain some wells which should all be negative to provide an estimate of the size of the background count. A common approach (see e.g. Langhorne and Fischer-Lindahl, 1981) is to select a threshold, often the mean plus two or three standard deviations of the background counts, and consider a well positive if its count exceeds this threshold. This approach clearly works well much of the time, as indicated by the straight lines frequently obtained when plotting the log of the frequency of negative wells against the number of cells per well. However, the background counts are usually not normally distributed about their mean, the more common situation being where there is considerable skewness, with the left-hand tail of the distribution being much shorter than its right-hand tail. Under these circumstances, reliance upon a threshold defined in terms of the mean and standard deviation of such counts can be problematic. This was the case with the data we consider in the present paper: determination of a threshold was not at all straightforward. A comparison of the counts corresponding to the wells in which no responding cells were expected with those for wells to which antigen was added revealed no clear cut-off in many cases. Efforts to develop more elaborate methods of determining the threshold for positive wells were not completely satisfactory. This led us to seek an analysis of the data which made direct use of the scintillation counts, and which did not reduce them to positive and negative well frequencies. There are good statistical reasons for avoiding the use of thresholds in situations where they are not entirely clear. In such cases, the actual threshold used can have a very great impact, indeed

be the dominant contributor to the final frequency estimates, yet the very real uncertainty in the determination of the threshold is typically not reflected in the standard errors or confidence limits given for these frequency estimates. Doing so presents formidable technical statistical problems, yet ignoring this important source of uncertainty can lead to quite unrealistic impressions concerning the precision of the frequency estimates.

There was a second, independent reason why it was desirable to avoid classifying wells as positive or negative: in many cases the entire set of wells for a given antigen would be positive. This arose whenever the density of cells chosen for the assay was a poor guess, something that could not always be avoided. In such cases the standard analysis of the data, given as a frequency of 100% of wells positive, does not yield a point estimate of the frequency of responding cells, but only a lower confidence limit. This causes difficulties later, when such results are to be compared or combined with other results. Since up to 20% of our assays would yield all positive wells, however the threshold was defined, we had a strong incentive to develop a method of estimating the frequency of responding cells another way. Similar remarks apply to the less frequent cases in which all wells would have been scored negative.

As with most studies of this kind, the approach we adopt below makes use of the Poisson model (PM) for the distribution of responding cells in a well. But instead of relating frequencies of responding cells to proportions of positive wells, we relate them to averages of suitably transformed scintillation counts. Our model involves plate-specific parameters which need to be estimated, but the evidence so far suggests that this can be done well enough to permit useful estimates of the frequencies of responding T-cells to be obtained from replicate pairs of microtiter plates involving cells at a single density. Full details are

given in the Methods section below, and in Appendix 1.

In order to demonstrate the validity of the new method, we analyse four LDAs on cells from three subjects, each involving three antigens and a control, carried out on replicate pairs of plates at six, five and four dilutions. We then compare the results obtained from a single dilution with those obtained using the entire LDA. We also analyse a number of assays run at a single dilution. As a further demonstration of the usefulness of this approach, we reanalyse the data from a quite different type of LDA, see Langhorne and Fischer-Lindahl (1981), namely a ^{51}Cr -release assay designed to estimate the frequency of cytotoxic T-lymphocyte precursor cells in mixed lymphocyte cultures. Finally, we analyse two additional proliferation assays of different designs to demonstrate the flexibility of this method: one a single density assay applied to samples pre- and post-immunization (S. Rodda, Chiron Mimotopes, Melbourne, Australia) and a set of three assays designed as limiting dilution assays (D. Koelle, University of Washington, Seattle, WA).

2 Materials and methods

2.1 Vaccine, antigens and subjects

Two subjects (#711 and #713) in a clinical trial of an HSV vaccine provided informed consent for the collection of additional blood for development of the assay. These subjects had never been infected with either HSV-1 or HSV-2 prior to vaccination with a vaccine consisting of 30 μg each of two HSV glycoproteins (D and B) expressed as a recombinant product in Chinese hamster ovary (CHO) cells. The proteins were combined with an oil-in-water emulsion

adjuvant (MF59, Chiron Corporation) and administered by intramuscular injection in the deltoid muscle at 0, 1 and 6 months (Langenberg et al., 1995). A third subject (NIH 1394) who was subject to frequent recurrences of genital herpes and who is HSV-2 positive was also recruited (Kost et al., 1993). The gD and gB proteins used in the assay were from the vaccine lots or comparable lots manufactured by Chiron Biocine (Emeryville, CA). Tetanus toxoid was a gift from Wyeth Laboratories (Nutley, NJ). Phytohemagglutinin was purchased from Sigma (St. Louis, MO).

2.2 Preparation of cells

Peripheral blood mononuclear cells (PBMC) were collected from the two vaccine study subjects 60–69 days after the third immunization by three pass leukapheresis. PBMC were prepared from the third subject by one pass leukapheresis. The recovered cells were further purified by density centrifugation onto Ficoll-Hypaque (Pharmacia), washed free of separation medium and prepared for cryopreservation in RPMI 1640 medium containing 20% pooled human serum and 7.5–10% DMSO. The cells were stored in multiple aliquots in vapor-phase liquid nitrogen until assay.

2.3 Description of the assays

Six point LDAs of PBMC from subjects #713 and #711 and a second 5 point LDA of PBMC from subject #713 were set up using information obtained from a frequency analysis assay (Reece et al., 1994a; M. Tigges, unpublished observations). PBMC from #713 contain a high frequency of gD2 and gB2 specific T-cells while #711 PBMC responded poorly to these two antigens.

The expected frequencies were 100 and 200 responders per 10^6 PBMC to gD2 and gB2 respectively from #713 and 5 and 2 responders per 10^6 PBMC to gD2 and gB2 respectively from #711. The frequency of gB2 and gD2 responsive T-cells in the NIH 1394 sample was expected to be on the order of 20–40 per 10^6 PBMC based on the results of assays with PBMC from HSV-2 seropositive subjects in other trials.

The PBMC were thawed and washed free of preservative with LGM-1 (RPMI 1640, JRH Biosciences, supplemented with 1 mM Na pyruvate, JRH Biosciences, 5 mM HEPES pH 7.2, Gibco, 2 mM glutamine, JRH Biosciences, 50 μ g/ml gentamicin, Gibco, and 1% pooled human serum). The pooled human serum (PHS) was prepared from screened units of recovered plasma. The washed cells were resuspended in lymphocyte growth medium containing 10% PHS (LGM-10), the cell concentration was adjusted, and the appropriate volume of the cell suspension was placed in the culture plates. The test antigens consisted of gD2 and gB2 at a concentration of 1 μ g/ml in 48 wells each distributed between two plates at each concentration. The control antigen consisted of Tetanus toxoid at 2 Lf/ml in 44 wells and the control mitogen, PHA, was added to two wells on each plate. The PBMC from subject #711 were seeded into U-bottom plates and those from subjects #713 and NIH 1394 were seeded into V-bottom plates. For U-bottom plates, the test and control antigens were diluted to 10 μ g/ml in LGM-10 then 20 μ l were transferred to the appropriate wells. The #711 PBMC were diluted into three cells suspension with densities of 10^6 , 5×10^5 and 2×10^5 cells/ml then either 200 or 150 μ l of the suspension were transferred to two plates. For PBMC from subject #713, the washed cells were adjusted to 10^5 cells/ml in LGM-10 then mixed with an equal volume of LGM-10 containing the test and control antigens at

2 $\mu\text{g}/\text{ml}$. The cells were then seeded into 48 replicate V-bottom wells in volumes of 150, 100, 75, 50, 35 and 25 μl . In a second assay the #713 cells were prepared similarly. The cells were resuspended at 5×10^5 cells/ml and seeded into replicate V-bottom wells in volumes of 100, 80 or 60 μl or resuspended at 2×10^5 cells/ml and seeded in volumes of 100 or 50 μl . The assay design for the NIH 1394 PBMC differed slightly in that the antigens and cells alone were seeded into 36 wells distributed over three plates (12 wells/plate); the Tetanus toxoid was included in only 6 wells and the PHA in 3 wells. After the cells were diluted for dispensing into the wells, a sample was taken to determine the actual number of cells seeded per well. All of the microwell plates were cultured for four days in humidified boxes at 37°C in 7% CO_2 before being labeled for six hours with 0.5 $\mu\text{Ci}/\text{well}$ of ^3H -thymidine. PHA was added to the appropriate wells on day 2. The plates were harvested using a Cambridge Technologies automated harvester and the filters counted in a Wallac/Pharmacia beta-plate scintillation counter.

The assay design for the data from S. Rodda was similar to that described above, except that 64 replicates were plated for each antigen tested and cells were plated at 200,000 cells/well. The PBMC were obtained from a single individual before and 3 weeks after immunization with Tetanus toxoid (Reece, et al., 1994a). The assays included preimmune cells, post-immunization cells, and a 1:1 mixture of the two. Test antigens included influenza ribonucleoprotein and a peptide that includes an epitope from Tetanus toxoid that is recognized by CD4^+ T-cells from many individuals (Reece, et al., 1994b). The data from D. Koelle were taken from an LDA design that consisted of 10,000 irradiated autologous PBMC/well, a graded number of between 50,000 and 780 PBMC and HSV-2 viral antigen in 24 replicates. The cells alone controls

were seeded in replicates of 12 or 24 on plates separate from the antigen containing wells. The cells were cultured for 5 days before being labeled with ^3H -thymidine and harvested on day 6.

2.4 Description of the data analysis

Our analysis of the data from a single microtiter plate makes use of all but two of the counts for the 96 wells: we do not use the counts for the two wells with PHA, which simply serve as a positive control for helping select usable data. We will describe the analysis of data from a single plate first, although our final analysis involves replicate pairs of plates.

The analysis is based upon the same PM that underlies most LDAs, but we need an extra relationship connecting the scintillation count to the number of responding cells in a well. Specifically, we suppose that there are plate-specific parameters a , b and σ , and a widely-applicable power parameter p such that the p th power of the scintillation count in a well with k responding cells is approximately normally distributed with mean $a + bk$ and standard deviation σ . As with other analyses using the PM, we suppose that the number of responding cells in a well with c PBMC is Poisson distributed with mean $fc \times 10^{-6}$, where f is the frequency of responding cells per million PBMC. Since we have 24 wells with cells alone, 24 with gD2, 24 with gB2 and 22 with Tetanus toxoid in any given plate, there will be 4 frequencies and 3 additional parameters for each plate. When we analyse replicate pairs of plates, there will be 10 parameters: the frequencies of each of the 4 classes of responding cells, assumed the same in each plate, and a set of 3 plate-specific parameters a , b and σ for each plate.

Algebraically, our assumptions are as follows. Let y_{ij} denote the transformed scintillation count for well j of class i , and let k_{ij} denote the corresponding number of responding cells. Here $i = 1, 2, 3, 4$ corresponds to the cells alone, gD2, gB2 and Tetanus toxoid classes, respectively. We assume that the (y_{ij}, k_{ij}) are mutually independent, that k_{ij} follows a Poisson distribution with mean λ_i , and that, given k_{ij} , y_{ij} follows a normal distribution with mean $a + bk_{ij}$ and standard deviation σ . The aim of our analysis is to estimate the parameters λ_i , and hence, using the estimated numbers of cells per well, the frequencies f_i of responding cells per million PBMC.

An initial plotting of the mean scintillation count across each set of wells against PBMC frequency was used to see if there was sufficient information in the count for analysis under this model to be feasible. We then turned to the estimation of the power parameter. It was selected by maximum likelihood from the values 1, 1/2, 1/4 and 0 (corresponding to log). The suitability of the normality assumption was examined by carrying out a Q-Q plot (Venables and Ripley, 1994) of the estimated residuals. The model itself was fitted by the method of maximum likelihood, specifically, using a form of the so-called EM algorithm (Dempster et al., 1977), although we also carried out a number of confirmatory analyses using the fully calculated likelihood. Standard errors for the parameter estimates were computed using the SEM algorithm (Meng and Rubin, 1991). We refer to Appendix 1 for full details of the algorithms used to carry out the analysis.

A by-product of the EM algorithm, which regards the “complete” data for any well as a pair (y, k) , where y is the observed scintillation count, and k the unobserved number of responding cells, is an estimate of k for each well. These can be plotted against the count, and provide an informative diagnostic for the

analysis of a plate. In particular, one can usually see the effective threshold distinguishing wells with no estimated responding cells from those with one or more.

The foregoing analysis provides estimates of the frequencies λ_1 , λ_2 , λ_3 and λ_4 of responding cells *per well* for each of the four classes: cells alone, gD2, gB2 and Tetanus toxoid. We next obtained MLEs of the frequencies of responding cells per well *above background*, i.e. of $\lambda_2 - \lambda_1$, $\lambda_3 - \lambda_1$ and $\lambda_4 - \lambda_1$, and then converted the resulting figures to frequencies per 10^6 cells. This last step involved scaling by the estimated number of cells/well in each plate, and the errors associated with such estimation are discussed in detail in Appendix 2. We note that as long as $\hat{\lambda}_2$, $\hat{\lambda}_3$ and $\hat{\lambda}_4$ are all $\geq \hat{\lambda}_1$, the MLEs of the differences $\lambda_2 - \lambda_1$, etc., are just the differences $\hat{\lambda}_2 - \hat{\lambda}_1$, etc., of the MLEs. In the rare cases where one or more of $\hat{\lambda}_2$, $\hat{\lambda}_3$ and $\hat{\lambda}_4$ was $\leq \hat{\lambda}_1$, a slightly modified analysis was necessary, involving combining sets of counts. The details are straightforward, see e.g. Barlow et al. (1972), and will be omitted.

In order to analyse the ^{51}Cr release assay, which has a more standard structure, with 24 replicate wells at each of 8 concentrations, we used the same basic method, modified to correspond to only a single unknown frequency of responder cells at each concentration.

The single density assay using data from S. Rodda consisted of six plates with cells from one subject taken before and after Tetanus immunization: a pair of plates with 200,000 preimmune cells per well, a pair with 200,000 post-immunization cells per well, and a pair containing a mixture of 100,000 preimmune cells per well and 100,000 post-immunization cells per well. Each plate consisted of three groups of 32 wells containing cells alone, cells treated with influenza RNP antigen, and cells treated with an epitope from Tetanus

toxoid, respectively. For each pair of plates, we estimate the frequency of responding cells per well for the three groups of wells (denoted λ_c , λ_t and λ_i , corresponding to cells alone, Tetanus, and influenza RNP, respectively), and two sets of plate-specific parameters (a, b, σ) .

The data from D. Koelle consist of three seven-point LDAs, corresponding to three different subjects. For each LDA, four plates were used. On the first plate, 24 wells were dedicated to each of four cell densities: 50,000, 25,000, 12,500 and 6,250 cells per well; antigen was added to each well. On the second plate, 24 wells were dedicated to each of three cell densities: 3,125, 1,563 and 781 cells per well; again, antigen was added to each well. The third and fourth plates in each LDA were like the first two, but with no antigen added. We analysed these data using the first and third plates together, with the parameters (a, b, σ) constrained to be equal for the two plates. The second and fourth plates were analysed similarly.

3 Results

In Table 1 we exhibit the scintillation counts for the duplicate pair of microtiter plates having cells from subject #713 at density 11,400 cells/well. Wells in columns 1–3 contains cells alone; wells in columns 4–6 contain cells together with the gD2 antigen; wells in columns 7–9 contain cells together with the gB2 antigen; while 22 of the 24 wells in columns 10–12 contain cells together with Tetanus toxoid, and wells A12 and B12 contain cells together with PHA. This is a typical set of data for two plates, and will be used below for illustrative purposes.

Figure 1 consists of plots of mean scintillation counts against cell density

for each of the five classes of wells, from one of the LDAs conducted on cells from subject #713. The vertical coordinate of each plotted point is a mean of the counts in 24 (for cells alone, gD2 and gB2), 22 (for Tetanus toxoid) or 2 (for PHA) wells, from one of the two microtiter plates, while the horizontal coordinate is the corresponding cell density. This figure strongly suggests that there is potentially usable information in the scintillation counts beyond that which helps classify a well as positive or negative. It shows a roughly linear relationship between mean scintillation count and the number of cells/well in all five cases. There is a tendency for this relationship to level off at high cell densities, particularly with the PHA and the Tetanus toxoid counts. Means of the square roots of the scintillation counts (data not shown, but see below) exhibit a slightly better linear relationship with cell density over the range seen with this assay. This linear relationship does not prove that the uptake of ^3H -thymidine is linearly related to the number of responding cells, but this seems to be a plausible conclusion, and it is on this foundation that our analysis is built. As we will see below, a square root transformation of the raw scintillation counts provides a better fit to the model than do the counts themselves.

Maximum likelihood estimates (MLEs) under the model (Finney, 1978) of the mean number of responding *cells/well* for the data in Table 1 are presented in Table 2, together with MLEs of the parameters a , b and σ and estimated standard deviations (SDs) for each estimate. We used the square root of the scintillation count, see below. Estimates were obtained by treating each plate *separately*, and also for the *joint* analysis of the pair of plates, where the mean numbers of responding cells/well were constrained to be equal. The estimated SDs given in parentheses after each parameter estimate take into account only

within-plate variation. No attempt has been made to include a component of variation between duplicates within duplicate pairs, and thus the SDs for the *joint* estimates are somewhat understated. The results for different members of a duplicate pair are usually quite close, and so this underestimation is unlikely to be a problem. When the two sets of results are quite different, it is usually the case that one of the pair is simply a bad plate, and the results are discarded. In any event, the variability between duplicates within duplicate pairs is usually very much smaller than the between-assay variability, as we shall see.

After obtaining estimates of the numbers of responding *cells/well* we calculate the frequency of *responding cells*/ 10^6 *cells* for each of the three antigens. The results for the first assay of subject #713 at density 11,400 cells/well are displayed in Table 3. In this table, these frequencies have been corrected for background using the estimated number of cells/well responding in the cells alone category. Furthermore, the estimated SDs presented incorporate variation due to cell counting and dilution errors, but between-assay variability is still not reflected in these SDs. It can be seen that at this stage our single dilution frequency estimates have coefficients of variation around 25%.

A by-product of the (EM) algorithm we use for maximum likelihood estimation is an estimate, for each well, of the number of responding cells in that well. These estimates are plotted against the square-root of the scintillation count and exhibited in Figure 2 for a selection of plates from three different assays. In Figure 2a (#713: 11,400 cells/well, plate 1, data in Table 1) we see that wells with counts less than 400 (20 on the square root scale) have been assigned 0 responding cells, while wells with counts greater than 900 (30 on the square root scale) have been assigned ≥ 1 responding cell. In between 400

and 900 is a grey area: there is no clear cut-off for this data. The mean and SD of the untransformed counts are 461 and 401 respectively, and so use of mean + 2SD as cut-off would lead to a figure of 1,263. It is evident that at least two, perhaps three wells in the cells alone group seem to contain a responding cell. Their scintillation counts inflate the SD of the cells alone counts, which in turn can lead to an unduly large cut-off under the traditional analysis of such data. In this case the count of 1,090 in well G1 would be classified as negative under the mean + 2SD rule, while for our analysis it is a positive well. Although this is only a single well, the ultimate classification of G1 could have a significant impact on estimates of frequencies of responding cells, and as noted above, the uncertainty over cut-offs is seldom, if ever, reflected in the SDs or confidence intervals calculated for frequency estimates.

In Figure 2b (#713: 1,990 cells/well, 2nd plate) we can see quite clearly the ranges of scintillation counts corresponding to estimates of 0, 1, 2 and 3 responding cells in a well, under the model. Figure 2c (#711: 155,200 cells/well, 1st plate) shows that when the number of responding cells in a well can be large, up to 10 or 11 in this case), the estimated relation between this number and the transformed scintillation count is a “broken stick” straight line. It is important to remember that this linear relation is not a validation of the model. We do not know (and cannot know in this context) the number of responding cells in any well: what we plot is the inferred or estimated number of such cells, on the assumption that the model is appropriate. In practice, we get results like those in Figure 2a–2c when the number of responding cells and the number of cells per well are not both large. Figure 2d (#713, 25,067 cells/well, 1st plate) shows what can happen when both numbers are large. The maximum-likelihood estimation involves trade-offs between the estimates

of frequencies of cells responding in the cells alone group and to antigens, and estimates of the plate-specific parameters a , b and σ , which define the relationship between the scintillation counts and the number of responding cells. It is not surprising that in very “crowded” conditions — high numbers of responding cells, high densities of cells/well, V-bottom wells — unusual things happen. The phenomenon exhibited in Figure 2d seems to be a consequence of the estimated value of σ being large in relation to that of b , for in such cases we cannot clearly distinguish “signal” (counts due to responding cells) from “noise” (variation about expected counts).

We now consider the evidence supporting our choice of the square-root of the scintillation counts as the most appropriate power transformation for the model as we structured it. Before we do this, however, a comment about our model is in order. The Poisson assumption for the number of responding cells in a well is made in line with most other writers on this and related assays, and we will comment more on this issue below. On the basis of Figure 1 we have proposed that within each well on a single plate a suitable transformed scintillation count is linearly related to the number of responding cells in that well, and, furthermore, the variation about the line is adequately described by the normal distribution. The latter is purely an assumption of convenience, for it permits the use of ordinary least-squares at the M-step of our iterative algorithm leading to the MLEs of all parameters. Our view was and is that provided there is no clear evidence of the inappropriateness of this assumption, once the power transformation is found which makes it most plausible, then the results of our analyses — their utility, reproducibility and consistency with other approaches — are the basis upon which the approach should be judged, not the validity of the precise details of the model.

With that preamble, we turn to Table 4 which displays the re-centred maximized log-likelihoods following power transformations of 1 (untransformed), $1/2$ (square root), $1/4$ (fourth root) and 0 (natural logarithm) of the scintillation counts. As can be seen from Table 4a, the best power transformation for the two assays of subject #713 ranges from $p = 1$ (untransformed) for the highest density of cells (31,333 cells/well), through to the $p = 0$ (natural log) for the lowest density (1,990 cells/well). It is clear that if a single transformation is to be used with these assays, and this is highly desirable, then $p = 1/2$, corresponding to the square root of scintillation counts, is best for the widest range of densities. The estimates of frequencies of responding cells do differ significantly according to the transformation used, which is why a widely-applicable transformation should be selected and used for a given, stable assay of this kind. The appropriateness of the square root transformation is further supported by noting the corresponding result in Table 4b for the dilution series involving subject #711: $p = 1/2$ is most frequently the best of the four transformations in that case as well.

A second line of evidence supporting the square root transformation can be found in the Q-Q plots of Figure 3. There the ranked scaled residuals $r = (y - \hat{a} - \hat{b}k)/\hat{\sigma}$ (for all plates in the LDAs #713 and #711) are compared to standard normal quantiles for each of the four power transformations considered here. When the model fits well, this Q-Q plot should be a straight line with slope 1, perhaps having a few outliers at either end. A comparison of the four plots shows that these conditions are best achieved with the scaled residuals based upon fitting the model to the square root transformed counts. (We point out that this conclusion is not wholly independent of that obtained from the Box-Cox analysis, but the linearity of the plot was *not* a foregone conclusion.)

In Table 5 we display the parameter estimates obtained by fitting the basic model to each plate separately. The data comes from the two LDAs of subject #713, and the single LDA from subject #711. In this table we can see the variation of parameter estimates between similarly treated pairs of plates, between dilutions, and between assays (first six vs. last five of #713) of the same stored sample. For example, we can see that both of the plates at 25,067 cells/well for #713 have a high σ to b ratio, as does the first plate at 31,333 cells/well.

The main results of our analysis have frequencies constrained to be equal across duplicate plates, while permitting the plate-specific parameters to vary. These are presented in Tables 6 and 7 for all samples of cells from subjects #713, #711 and NIH 1394. Table 6 gives the frequencies as numbers of cells/well responding to antigen, after adjusting these for the frequency of responding cells in the cells alone group. By contrast, Table 7 presents the results as frequencies of responding cells per million cells. This variant requires an estimate of the number of cells in each well, and there can be substantial sampling error in such estimates. In order to display the impact of such errors on the precision of the estimated frequencies, we have included two standard deviations with each estimate, one (SD) which does not, and the other (SD_a) which does take into account this component of error. It can be seen that the resulting coefficients of variation (CV_a) are largely in the 10%-25% range, although they can get as high as 36%, and are undefined when the estimate of frequency of responding cells is 0.

We turn now to the results which show the performance of the assay using single dilutions. In Table 8 we present the estimated plate parameters for the four LDAs discussed in this paper. The way in which a , b and σ vary with

the number of cells/well within and between assays can then be seen. In order to avoid cluttering up this table, we have not displayed the estimated SDs of the parameter estimates presented, but those given in Table 2 are typical. As explained in Section 3 above, each plate in NIH 1394 contains cells at all four dilutions used in that assay. A number of features of this table are worthy of note. Firstly, there is a clear relationship between the estimated value of the parameter a and the number of cells per well within each of the first two assays, with higher cell densities corresponding to higher estimated values of a . By contrast, the estimated values of b and σ show no clear trend with cell density, nor does the a for #713, assay 2. Secondly, the estimated magnitudes of a , b and σ vary markedly between assays, suggesting that these parameters are not only plate specific, within assays, but to some extent assay specific. Thirdly, we see that for the most part, the parameter σ lies in the range from $b/3$ to $b/2$, although at times σ can be approximately equal to b (#713, assay 2, plate 1; NIH 1394, assay 2), or even greater (#713, assay 2). This last phenomenon should be regarded as a failure of the model with data from these plates.

In Figure 4, estimates of the frequencies of responding cells per 10^6 cells are plotted against cell density, with error bars corresponding to ± 1 SD. Here the SD incorporates both within plate variation and errors involved in counting the number of cells/well and dilution errors (see Appendix 2). The dotted line in each plot corresponds to the estimated frequency of responding cells/ 10^6 cells obtained by carrying out a maximum likelihood analysis using all the data from both LDAs, but not the single assays. It is immediately clear from Figure 4 that the error bars we have calculated understate the variability exhibited by the estimates. Roughly speaking, we would expect about 68% of these $+/- 1$ SD intervals to contain the true (but unknown) frequency, if they

incorporated *all* sources of variability, and it seems evident that this is unlikely to be the case. In particular, the intervals given in the second assay for #713 at the three highest cell densities, and those for the antigens gD2 and gB2 at the four highest cell densities for #711, seem too small by perhaps a factor of 2. Despite these difficulties with the estimation of error, it is apparent that the use of these assays at a single carefully chosen density of cells will yield estimates of the frequency of responding cells with a coefficient of variation of the order of 20% – 25% or better.

In order to re-analyse the data from Langhorne and Fischer-Lindahl (1981), it was first necessary to read the counts per minute ($\times 10^{-2}$) from their Figure 2. The values we obtained and used are presented in Table 9. In Table 10 we exhibit the MLEs of the CTL-precursor frequencies for each cell density, and also the associated estimates of plate-specific parameters. As before, the SDs reflect only within-plate variation. Figure 5 shows these estimates plotted against the number of responders, where the estimates from the traditional analysis are also presented. Note that for these data, the untransformed scintillation counts were used, as indicated by a Box-Cox analysis.

The effectiveness of our analysis of the CTL-precursor assay data from Langhorne and Fischer-Lindahl (1981) is evident from Figure 5. Not only do our estimates of the CTL-precursor frequencies give a slightly better linear relation than the traditional ones, based upon the first 6 frequencies, our estimates of b and σ were remarkably stable over this range, while the estimates of a increase with cell density, as we saw above. It is worth pointing out that we have analysed these data as though the different sets of 25 counts at each precursor cell density were obtained from different microtiter plates, estimating a new a , b and σ for each set. It is not clear from the paper whether this was

the case, but if not, then an analysis constraining some of the plate-specific parameters to be equal would be both more appropriate and more efficient.

Table 11 presents the results of our analysis of the data from S. Rodda. Here λ_c , λ_t and λ_i denote the estimated frequencies of responding cells per well for the cells alone, Tetanus and influenza RNP groups, respectively. For these data, the square roots of the scintillation counts were used. Note that the estimated frequency for the 50:50 mixture is the approximately the average of the estimated frequencies of its components, within the estimated error.

Table 12 presents the results of our analysis of the data from three LDAs from D. Koelle, while Figure 6 gives a plot of the estimated frequencies of responding cells per well (above background) against cell density. We notice that although there appears to be a reasonable linear relationship between estimated frequency of responders and number of cells per well, the estimated ratio of b to σ for two pairs of plates (DK2, #2,4; KD, #2,4) suggests difficulty fitting the model, while those for two other pairs (DK2, #1,3; EL, #1,3) are only marginally satisfactory.

4 Discussion

The main objective of our analysis was to obtain estimates of frequencies of responding cells based upon a single dilution. It is clear from the results in Table 7 and Figure 4 that we can do this with a coefficient of variation of about 30% or lower, apart from a component of assay-to-assay variation which we discuss shortly. But before doing so, we recall the stated aim of our single dilution assay: it was intended to be a significantly more sensitive version of the standard proliferation assay, which obtains a “stimulation index” as

the ratio of the mean scintillation count from three test wells to the mean count from three wells with cells alone. Our assay was not intended to be a replacement for a standard LDA, whether analysed in the usual way by reducing the well counts to quantal responses, or under the model presented in this paper, although it does seem that our model and analysis will provide an alternative, possibly more efficient analysis of such LDAs, under certain circumstances. We have presented analyses of a variety of full LDAs simply to enable us to assess the extent to which our single dilution estimates can be relied upon.

Between assay variation is clearly an important issue, and its extent can be gauged from Table 7 and Figure 4. Apparently it can be quite substantial, with the results for Tetanus toxoid being of particular concern. It might therefore be thought essential that the SDs assigned to frequency estimates should incorporate a component of between-assay variation, so that we get a realistic impression of the true imprecision in these estimates. The issue is not a simple one, however, as there are many contributors to between-assay variation, not all of which operate to the same extent in each new assay. For example, replicate assays carried out by the same experienced technician will typically lead to more concordant frequency estimates than would be obtained with different, or less experienced technicians. The quality of the thawed cells can vary in unpredictable ways, with time since freezing being an important factor, and the reagents used in the assay can also affect the frequencies obtained. We feel that this topic is best studied within the context of a larger ongoing trial, in which some samples are routinely analysed in two or more different assays. For this reason we will not discuss the matter any further here, apart from noting that on the basis of the evidence presented here, it

might not be unreasonable to double the estimated SDs of frequency estimates if between-assay variation is to be incorporated.

The method of analysis we have presented in this paper highlights certain issues relating to the design of assays of the kind we discuss. The most important concerns the relation of the negative control wells, our cells alone, to wells containing antigen. We have examined and analysed a number of assays in which the negative control wells and the wells containing antigen were located on different microtiter plates. Although this practice is not necessarily injudicious, there are at least three reasons why it should be avoided, particularly if our method of analysis is to be used, but even more generally. As is made explicit by our estimation of the plate-specific parameters a , b and σ , the responses of cells from the same source can differ from plate to plate, even in well-conducted assays. It is good general practice to carry out comparative analyses with the greatest possible degree of control over the conditions which could cause differences, in this case, between negative control and antigen wells, for the responses in wells with antigen will be adjusted to the extent that the negative control wells respond. If it is not possible to make such intra-plate adjustments, it becomes necessary to assume that the plate containing the negative control wells has the same parameters as that containing the wells with antigen, for otherwise the two classes of wells will not be treated similarly in their analysis.

Further, it may not be possible to estimate all the parameters in our approach, for our method relies upon there being a certain level of variation in response in order to ensure what is known as the identifiability of the parameters. To take an extreme, but by no means unusual situation, suppose that all the negative control wells were together on their own plate, and that there

were no responding cells in this case. Then it is clearly impossible to estimate a non-zero frequency of responding cells, and equally there will be no way to estimate anything more than the average background count (our a) and the variation (our σ) about it; the increase in count per responding cell (our b) is not estimable. Further, in order to use these results to adjust the responses from a plate with the antigen containing wells, we would have to assume that the conditions (our a and σ) are the same for both plates, whereas with a design which had negative controls in both plates, this further assumption would be unnecessary.

We close with some comments concerning the model and its validity. Firstly, there is the question of the interpretation of our parameters and the range of reasonable values for them. The parameter a is most easily interpreted as the average or median value of the counts or transformed counts observed in the wells in the cells alone category. Of course it will also have the same relation to the counts from those wells with antigen in which there are no responding cells, but we will not usually know definitely which these are, whereas we can generally be confident that the overwhelming majority of counts from wells in the cells alone category are simply background. The parameter b is the slope of the line relating average count or transformed count to frequency of responding cells within a plate. We can typically obtain 4 such points, corresponding to the 4 groups of wells. (The mean count or transformed count for a group with λ responding cells/well is $a + b\lambda$, which, when plotted against λ , has slope b .) Finally, the parameter σ corresponds to the spread of counts or transformed counts about their mean, for wells with the same number of responding cells. Under our normality assumption, about 95% of such counts would be within 2σ of the mean, which has the form $a + kb$. Thus satisfactory

discrimination between adjacent values of k is only possible when σ is $b/2$ or smaller, and is really good if $\sigma \leq b/4$. Our algorithm can converge and give reasonable frequency estimates with values of σ as large as b , or even larger than b . However, we are inclined to regard such situations as failures of the model to fit the data, and include them only when there is no other way to get a frequency estimate, and a rough one is desired.

The appropriateness of our use of the Poisson distribution could also be questioned. This is a natural and convenient assumption, but it is hard to produce strong evidence of its validity. The linearity of estimates in an LDA, when plotted against the number of cells per well, is suggestive, and its absence would disconfirm the assumption, but not much more can be said without large high quality data sets. We believe that the widespread and usually satisfactory application of the SHPM has a similar justification. Few, if any studies exist offering detailed justification of this model. Indeed it is not an easy model to refute, as many quite differently motivated models (two-hit Poisson, helper two-target Poisson, suppressor two-target Poisson, etc.) can give rather similar results to those obtained under the SHPM, and would require quite high-quality data and appropriate tests to be distinguished from the SHPM (Bonnefoix and Soto, 1995).

A question which arises naturally with our analysis is the dependence of our conclusions on the normality assumption, and the robustness of this assumption. In another paper (Broman et al., 1995), we have discussed a non-parametric alternative to the current model, in which the normal distribution for the residual $y - (a + bk)$ is replaced by an arbitrary symmetric distribution. In that same paper a robust estimation procedure is discussed, based upon empirical characteristic functions. What was striking about the analysis given

there for the LDAs for subject #713, was how close the parameter estimates obtained were to those found under the normal model. This was not just so for the estimates of the frequencies of responding cells, but also for the parameters a and b . (In the nonparametric model there is no parameter σ .) We conclude that the normality assumption, and its robustness are not important issues for the data we have discussed here.

Our model is a form of mixture model, and with all such models, one must take care to ensure that the estimates used are not those corresponding to local maxima of the likelihood, but are genuine maximum likelihood estimates. The steps we took to ensure this could certainly be strengthened, but what we did was as follows. First, we chose a cut-off point for the scintillation count of wells containing no responding cells. Using this cut-off, it is straightforward to obtain estimates of the parameters λ , and then (as described earlier) the parameters a , b and σ . Next, we picked a number of points at random from the parameter space, centered at our rough estimate. Starting at each of these points, we ran the EM algorithm until convergence to a local maximum, and calculated the value of the likelihood at the local parameter combination obtained. The parameters corresponding to the largest local maximum are then taken. Simulations (data not shown) have reassured us that this approach works well with data of the kind we have discussed in this paper.

There is a definite gain in efficiency in the estimates of the parameters λ when one uses the analysis we have described, rather than the traditional one based upon classifying the wells as positive and negative, even when this can be done essentially without error. As one might expect, this gain is not so great when the mean number of responding cells/well is small, such as unity or smaller, but it can be significant when the mean number of such cells is

substantially greater than unity. As an indication of the possible gains, we offer the results in Table 13. This table gives estimates and estimated SDs for five of the cell densities of the Langhorne and Fischer-Lindahl data, along with a joint analysis, using both the cut-off method and our new method. Also given are the ratio of the estimated variances for the two methods, which indicates the improvement obtained by the new method.

Finally, we remark that our model and analysis, originally designed for the particular assay described in the Methods section, does appear to have a wider usefulness. With only relatively minor adaptations, it could be applied to the CTL-precursor assay of Langhorne and Fischer-Lindahl (1981), as well as to data from LDAs (D. Koelle), and the single density assay of S. Rodda, all of which had a structure quite different from that of the original assays. In each case analysis gave satisfactory results, and in a way which avoided the arbitrary choice of cut-offs. Assuming that the model we used is appropriate, our analysis will also be more efficient.

5 Acknowledgements

Many thanks are due to David Freedman and Peter Hall for their helpful comments on the material in this paper. We also wish to thank Mario Geysen and Stuart Rodda for the initial application of the single cell density and for many helpful discussions in the early development of the frequency analysis.

6 References

- Barlow, R. E., Bartholomew, D. J., Bremner, J. M. and Brunk, H.D. (1972) Statistical inference under order restrictions; the theory and application of isotonic regression. Wiley, New York.
- Bonnefoix, T. and Soto, J.-J. (1994) The standard χ^2 test used in limiting dilution assays is insufficient for estimating the goodness-of-fit in the single-hit Poisson model. *J. Immunol. Methods* 167, 21.
- Box, G. E. P. and Cox D. R. (1964) The analysis of transformations. *J. R. Stat. Soc., Ser. B* 26, 211.
- Broman, K. W., Hall, P. G., Jensen, J. L. and Speed, T. P. (1995) Methods for estimating the singular component of a distribution. In preparation.
- Cobb, L., et al. (1989) Comparison of statistical methods for the analysis of limiting dilution assays. *In Vitro Cell. Dev. Biol.* 25, 76.
- Cyr, L., et al. (1993) Confidence intervals for the relative frequency of responding cells in limiting dilution assays. *Biometrics* 49, 491.
- Dempster, A., Laird, N. and Rubin, D. (1977) Maximum likelihood estimation from incomplete data via the EM algorithm. *J. R. Stat. Soc., Ser. B* 39, 1.
- Finney, D. J. (1978) *Statistical method in biological assay*. Academic Press, New York.
- James, S. P. (1991) Measurement of basic immunologic characteristics of human mononuclear cells. In: J. E. Coligan, A. M. Kruisbeek, D. H. Margulies, E. M. Shevach and W. Stroger (Eds.), *Current Protocols in Immunology*.

- Green Publishing Company and Wiley–Interscience, New York. Section 7.10.
- Koelle, D. M., Abbo, H., Peck, A., Ziegweid, K. and Corey, L. (1994) Direct recovery of herpes simplex virus (HSV)-specific T lymphocyte clones from recurrent genital HSV-2 lesions. *J. Infect. Dis.* 169, 956.
- Kost, R. G., Hill, E. L., Tigges, M. and Straus, S. E. (1993) Brief report: Recurrent acyclovir-resistant genital herpes in an immunocompetent patient. *N. Engl. J. Med.* 329, 1777.
- Langenberg, A. G. M., Burke, R. L., Adair, S. F., Sekulovich, R., Tigges, M., Dekker, C. L. and Corey, L. (1995) A recombinant glycoprotein vaccine for herpes simplex type 2: Safety and efficacy. *Ann. Intern. Med.* 122, 889.
- Langhorne, J. and Fischer-Lindahl, K. (1981) Limiting dilution analysis of precursors of cytotoxic T-lymphocytes. *Immunol. Methods* 11, 221.
- Lefkovits, I. and Waldmann, H. (1979) Limiting dilution analysis of cells in the immune system. Cambridge University Press, Cambridge.
- Lefkovits, I. and Waldmann, H. (1984) Limiting dilution analysis of cells in the immune system. I. The clonal basis of immune response. *Immunol. Today* 5, 265.
- Meng, X.-L. and Rubin, D. B. (1991) Using EM to obtain asymptotic variance-covariance matrices: the SEM algorithm. *J. Am. Stat. Asso.* 86, 899.
- Nelder, J. A. and Mead, R. (1965) A simplex method for function minimization. *Computer J.* 7, 308.

- O'Leary, J. J., et al. (1980) Quantitation of [³H]-thymidine uptake by stimulated human lymphocytes. *Cell Tissue Kinet.* 13, 21.
- Parr, D., Savarese, B., Burke, R. L., Margolis, D., Meier, J., Markoff, L., Ashley, R., Corey, L., Adair, S., Dekker, C. and Straus, S. E. (1991) Ability of a recombinant herpes simplex virus type 2 glycoprotein D vaccine to induce antibody titers comparable to those following genital herpes. *Clin. Res.* 39, 216A.
- Reece, J. C., McGregor, D. L., Geysen, H. M. and Rodda, S. J. (1994a) Scanning for T helper epitopes with human PBMC using pools of short synthetic peptides. *J. Immunol. Methods* 172, 241.
- Reece, J. C., Geysen, H. M. and Rodda, S. J. (1994b) Mapping the major human T helper epitopes of Tetanus toxoid. The emerging picture. *J. Immunol.* 151, 6175.
- Rodda, S. J. and Geysen, H. M. (1991) *Pinnacles. Mimotopes*, Melbourne, Victoria, Australia.
- Rodda, S. J., Reece, J. C., Mutch, D. A. and Geysen, H. M. (1992) Exhaustive T helper cell determinant mapping with uncloned human peripheral blood mononuclear cells. II. Pooled peptides as antigens for screening. Unpublished observations.
- Straus, S. E., Savarese, B., Tigges, M., Freifeld, A. G., Krause, P. R., Margolis, D. M., Meier, J. L., Paar, D. P., Adair, S. F., Dina, D., Dekker, C. and Burke, R. L. (1993) Induction and enhancement of immune responses to

- herpes simplex virus type 2 in humans by use of a recombinant glycoprotein D vaccine. *J. Infect. Dis.* 167, 1045.
- Taswell, C. (1981) Limiting dilution assays for the determination of immunocompetent cell frequencies. I. Data analysis. *J. Immunol.* 126, 1614.
- Taswell, C. (1984) Limiting dilution assays for the determination of immunocompetent cell frequencies. III. Validity tests for the single-hit Poisson model. *J. Immunol. Methods* 72, 29.
- Taswell, C. (1987) Limiting dilution assays for the separation, characterization and quantitation of biologically active particles and their clonal progeny. In: T. G. Pretlow II and T. G. Pretlow, (Eds.), *Cell Separation Methods and Selected Applications*, Vol. 4. Academic Press, New York, p. 109.
- Venables, W. N. and Ripley, B. D. (1994) *Modern applied statistics with S-Plus*. Springer-Verlag, New York.

7 Appendix 1. EM and SEM algorithms

Here we describe our methods for obtaining parameter estimates and estimates of their standard errors. In Appendix 2, we describe our method for obtaining revised estimated standard errors which incorporate the errors in the cell counts and due to dilution.

Let y_{ij} denote the transformed scintillation count for well j of class i (where $j = 1, \dots, n_i$, $i = 1, \dots, 4$, and $n = \sum_{j=1}^4 n_i$), and let k_{ij} denote the (unobserved) number of responding cells in that well. We assume that the (y_{ij}, k_{ij}) are mutually independent, that k_{ij} follows a Poisson distribution with mean λ_i , and that, given k_{ij} , y_{ij} follows a normal distribution with mean $a + bk_{ij}$ and variance σ^2 . For simplicity, we write $\theta = (\lambda_1, \dots, \lambda_4, a, b, \sigma)$.

7.1 Maximum likelihood estimates

We use an implementation of the EM algorithm (Dempster et al., 1977) to obtain maximum likelihood estimates of the parameters θ . The EM algorithm is a useful approach in situations, such as ours, where the observations can be viewed as incomplete data, and where obtaining maximum likelihood estimates would be quite simple if one had observed the full data.

One begins with an initial estimate of the parameters. The algorithm is composed of two steps, which are performed iteratively. In the expectation or E step, one obtains the expected values of the full-data sufficient statistics, given the observed data and the current estimates of the parameters. In the maximization or M step, one obtains revised parameter estimates by maximization under the full likelihood, using the current expected values of the full-data sufficient statistics. We denote the arrays of (y_{ij}) and (k_{ij}) by y and

k respectively, and similarly λ denotes the vector (λ_i) .

Consider the full-data likelihood for our model:

$$\begin{aligned}
 L(\theta|y, k) &= p(y, k|\theta) \\
 &= p(k|\lambda)p(y|k, a, b, \sigma) \\
 &= \prod_{i,j} p(k_{ij}|\lambda_i)p(y_{ij}|k_{ij}, a, b, \sigma) \\
 &= \prod_{i,j} \frac{e^{-\lambda_i} \lambda_i^{k_{ij}}}{k_{ij}!} \frac{1}{\sigma\sqrt{2\pi}} \exp\left[-\frac{(y_{ij} - a - bk_{ij})^2}{2\sigma^2}\right]
 \end{aligned}$$

This is easily seen to correspond to an exponential family, with sufficient statistics $\sum_j k_{ij}$ (for $i = 1, \dots, 4$), $\sum_{i,j} y_{ij}$, $\sum_{i,j} y_{ij}^2$, $\sum_{i,j} y_{ij}k_{ij}$, and $\sum_{i,j} k_{ij}^2$.

Now, consider a single iteration of the EM algorithm. In the E step, we obtain the expected values of the above sufficient statistics given the y_{ij} and the current estimates of the parameters. We first calculate the expected value of k_{ij} and k_{ij}^2 , for each i, j . This is done numerically, using the following formulae (note that, for small λ s, it is sufficient to perform the sums for k up

to only 10 or 20):

$$\begin{aligned}
\mathbf{E}(k_{ij}|y_{ij}, \lambda_i, a, b, \sigma) &= \frac{\sum_{k \geq 0} k p(k|\lambda_i) p(y_{ij}|k, a, b, \sigma)}{\sum_{k \geq 0} p(k|\lambda_i) p(y_{ij}|k, a, b, \sigma)} \\
&= \frac{\sum_{k \geq 0} \frac{e^{-\lambda_i} \lambda_i^k}{k!} \frac{k}{\sigma\sqrt{2\pi}} \exp\left[-\frac{(y_{ij}-a-bk)^2}{2\sigma^2}\right]}{\sum_{k \geq 0} \frac{e^{-\lambda_i} \lambda_i^k}{k!} \frac{1}{\sigma\sqrt{2\pi}} \exp\left[-\frac{(y_{ij}-a-bk)^2}{2\sigma^2}\right]} \\
&= \frac{\sum_{k \geq 1} \frac{\lambda_i^k}{(k-1)!} \exp\left[-\frac{(y_{ij}-a-bk)^2}{2\sigma^2}\right]}{\sum_{k \geq 0} \frac{\lambda_i^k}{k!} \exp\left[-\frac{(y_{ij}-a-bk)^2}{2\sigma^2}\right]} \\
\mathbf{E}(k_{ij}^2|y_{ij}, \lambda_i, a, b, \sigma) &= \frac{\sum_{k \geq 0} k^2 p(k|\lambda_i) p(y_{ij}|k, a, b, \sigma)}{\sum_{k \geq 0} p(k|\lambda_i) p(y_{ij}|k, a, b, \sigma)} \\
&= \dots \\
&= \frac{\sum_{k \geq 2} \frac{k\lambda_i^k}{(k-1)!} \exp\left[-\frac{(y_{ij}-a-bk)^2}{2\sigma^2}\right]}{\sum_{k \geq 0} \frac{\lambda_i^k}{k!} \exp\left[-\frac{(y_{ij}-a-bk)^2}{2\sigma^2}\right]}
\end{aligned}$$

The expected values of the sufficient statistics are then calculated as follows:

$$\begin{aligned}
\mathbf{E}\left(\sum_j k_{ij} \middle| y, \lambda, a, b, \sigma\right) &= \sum_j \mathbf{E}(k_{ij}|y, \lambda, a, b, \sigma) \\
\mathbf{E}\left(\sum_{i,j} k_{ij}^2 \middle| y, \lambda, a, b, \sigma\right) &= \sum_{i,j} \mathbf{E}(k_{ij}^2|y, \lambda, a, b, \sigma) \\
\mathbf{E}\left(\sum_{i,j} k_{ij} y_{ij} \middle| y, \lambda, a, b, \sigma\right) &= \sum_{i,j} y_{ij} \mathbf{E}(k_{ij}|y, \lambda, a, b, \sigma) \\
\mathbf{E}\left(\sum_{i,j} y_{ij} \middle| y, \lambda, a, b, \sigma\right) &= \sum_{i,j} y_{ij} \\
\mathbf{E}\left(\sum_{i,j} y_{ij}^2 \middle| y, \lambda, a, b, \sigma\right) &= \sum_{i,j} y_{ij}^2
\end{aligned}$$

In the M step, we estimate λ_i by our current estimate of $\sum_j k_{ij}/n_i$, and we estimate a , b , and σ^2 by regressing the y_{ij} on the k_{ij} , using our current estimates of the full-data sufficient statistics:

$$\begin{aligned}\hat{b} &= \frac{\sum_{i,j} y_{ij} k_{ij} - (\sum_{i,j} y_{ij}) (\sum_{i,j} k_{ij}) / n}{\sum_{i,j} k_{ij}^2 - (\sum_{i,j} k_{ij})^2 / n} \\ \hat{a} &= \left(\sum_{i,j} y_{ij} - \hat{b} \sum_{i,j} k_{ij} \right) / n \\ \hat{\sigma}^2 &= \left(\sum_{i,j} y_{ij}^2 + n \hat{a}^2 + \hat{b}^2 \sum_{i,j} k_{ij}^2 - 2 \hat{a} \sum_{i,j} y_{ij} - 2 \hat{b} \sum_{i,j} y_{ij} k_{ij} + 2 \hat{a} \hat{b} \sum_{i,j} k_{ij} \right) / n\end{aligned}$$

To obtain our estimates, then, we begin with a set of initial estimates and iteratively perform the above E and M steps until convergence.

Note that the likelihood surface for the problem under consideration is generally multimodal. In order to ensure the achievement of the point at which the likelihood is globally maximized, or at least is close to a global maximum, it is necessary to perform the EM algorithm from a number of different starting points. To choose among the different points to which the algorithm converges, we explicitly calculate the observed-data likelihood at each of these points, and determine which gives the maximum likelihood. We may still not achieve the global maximum, but we feel that our choice of multiple starting points gives quite good results.

Our method of choosing starting points is as follows. Having transformed the scintillation counts, we use the cut-off method to estimate the λ_i : we choose a cut-off and then estimate $\hat{\lambda}_i = -\log(q_i)$, where q_i is the proportion of wells, in the i th group, which are below the cut-off. Our initial estimate

of a is the median of the transformed scintillation counts, among the wells below our chosen cut-off. Let m_i be the mean of the transformed scintillation counts for group i ; m_i should be around $a + b\lambda_i$, and so our initial estimate of b is the median (over all of the groups) of $(m_i - a)/\lambda_i$. Since we've found that σ is generally between $b/4$ and $b/2$, our initial estimate of σ is $\hat{b}/3$. Using this rough estimate, denoted $\hat{\theta}^{(\text{rough})}$, a number of additional starting points can be obtained, for example, by sampling u_i iid uniform $(-1, 1)$, and letting $\hat{\theta}_i^{(0)} = e^{u_i} \hat{\theta}_i^{(\text{rough})}$.

One might also obtain the maximum likelihood estimates by explicitly maximizing the observed-data likelihood (using, for example, the Nelder-Mead simplex method (Nelder and Mead, 1965)). For our model, the observed-data likelihood is as follows:

$$\begin{aligned}
L(\lambda, a, b, \sigma | y) &= \prod_{i,j} p(y_{ij} | \lambda_i, a, b, \sigma) \\
&= \prod_{i,j} \left[\sum_{k \geq 0} p(k | \lambda_i) p(y_{ij} | k, a, b, \sigma) \right] \\
&= \prod_{i,j} \left\{ \sum_{k \geq 0} \frac{e^{-\lambda_i} \lambda_i^k}{k_{ij}!} \frac{1}{\sigma \sqrt{2\pi}} \exp \left[-\frac{(y_{ij} - a - bk)^2}{2\sigma^2} \right] \right\}
\end{aligned}$$

7.2 Estimated standard errors

To obtain estimates of the standard errors of our estimated parameters, we use the fact that the asymptotic variance-covariance matrix satisfies $V = I_o^{-1}(\theta | y)$, where we write $\theta = (\lambda_1, \dots, \lambda_4, a, b, \sigma)$, and where $I_o(\theta | y)$ is the observed-data information matrix, obtained by calculating the matrix of second derivatives of the negative log likelihood.

Meng and Rubin have described a method, which they call the SEM algorithm (Meng and Rubin, 1991), for obtaining the above observed-data information matrix from the full-data information matrix, $I_o(\theta|y, k)$, and the rate of convergence of the EM algorithm. Using the notation of Meng and Rubin, we describe their SEM algorithm and its implementation for our problem.

The EM algorithm defines a map $\theta^{(t+1)} = M(\theta^{(t)})$, for which the maximum likelihood estimate, $\hat{\theta}$, is a fixed point, meaning $\hat{\theta} = M(\hat{\theta})$. Let DM denote the Jacobian matrix of M evaluated at $\hat{\theta}$, so that, if we let r_{ij} denote the (i, j) th element of DM , $r_{ij} = \frac{\partial M_j(\theta)}{\partial \theta_i} \Big|_{\theta=\hat{\theta}}$.

Let I_{oc} denote the expected value of the full-data information matrix, given the observed data, evaluated at $\hat{\theta}$, so that $I_{oc} = \mathbf{E} [I_o(\theta|y, k)|y, \theta] \Big|_{\theta=\hat{\theta}}$.

Meng and Rubin showed that the observed data asymptotic variance-covariance matrix, V , can be written as $V = I_{oc}^{-1} (I - DM)^{-1}$.

For our model, the full-data information matrix, $I_o(\theta|y, k)$, calculated by taking the second derivative of the full-data negative log likelihood, is as follows, where empty cells are to be filled in with zeros.

$$\left(\begin{array}{cccccccc} \frac{\sum_j k_{1j}}{\lambda_1^2} & & & & & & & \\ & \frac{\sum_j k_{2j}}{\lambda_2^2} & & & & & & \\ & & \frac{\sum_j k_{3j}}{\lambda_3^2} & & & & & \\ & & & \frac{\sum_j k_{4j}}{\lambda_4^2} & & & & \\ & & & & \frac{n}{\sigma^2} & & \frac{\sum_{i,j} k_{ij}}{\sigma^2} & \\ & & & & & \frac{\sum_{i,j} k_{ij}}{\sigma^2} & \frac{\sum_{i,j} k_{ij}^2}{\sigma^2} & \\ & & & & & & & \frac{3}{\sigma^4} \sum_{i,j} (y_{ij} - a - bk_{ij})^2 - \frac{n}{\sigma^2} \end{array} \right)$$

As Meng and Rubin describe, since $I_o(\theta|y, k)$ is a linear function of the sufficient statistics, the matrix I_{oc} can be calculated by evaluating $I_o(\theta|y, k)$ at the expected value of the sufficient statistics, found in the last E step of the EM algorithm, and at the maximum likelihood estimate, $\hat{\theta}$.

Let r_{ij} denote the (i, j) th element of the matrix DM , and let $\hat{\theta}$ denote the MLE of θ . Then

$$r_{ij} = \lim_{\theta_i \rightarrow \hat{\theta}_i} \frac{M_j(\hat{\theta}_1, \dots, \hat{\theta}_{i-1}, \theta_i, \hat{\theta}_{i+1}, \dots, \hat{\theta}_7) - \hat{\theta}_j}{\theta_i - \hat{\theta}_i}$$

Thus the matrix DM can be calculated as follows.

1. Calculate the MLE, $\hat{\theta}$, using the EM algorithm.
2. Pick a starting point, $\theta^{(0)}$, some small distance from $\hat{\theta}$.
3. Repeat the following until convergence.

- (a) Calculate $\theta^{(k)} = M\theta^{(k-1)}$, using one step of the EM algorithm.
- (b) For each $i = 1, 2, \dots, 7$,
- i. Let $\theta^{(k)}(i) = (\hat{\theta}_1, \dots, \hat{\theta}_{i-1}, \theta_i^{(k)}, \hat{\theta}_{i+1}, \dots, \hat{\theta}_7)$. (Replace the i th element of $\hat{\theta}$ with the i th element of $\theta^{(k)}$.)
 - ii. Perform one step of the EM algorithm on $\theta^{(k)}(i)$, to obtain $M[\theta^{(k)}(i)]$.
 - iii. Let $r_{ij}^{(k)} = \{M_j[\theta^{(k)}(i)] - \hat{\theta}_j\} / \{\theta_i^{(k)} - \hat{\theta}_i\}$.

As suggested by Meng and Rubin, we allow the r_{ij} to converge at different rates. The element r_{ij} is taken to be the first value of $r_{ij}^{(k)}$ which satisfies $|r_{ij}^{(k)} - r_{ij}^{(k-1)}| < \epsilon$, where ϵ is some chosen tolerance value, and where the k at which we stop is allowed to depend on (i, j) .

8 Appendix 2. Cell count errors

8.1 Method for obtaining cell counts

We start with a blood sample with a cell concentration of X cells per ml. A $100 \mu\text{l}$ aliquot of this sample is combined with $100 \mu\text{l}$ of Trypan blue dye and is placed in a hemacytometer, which takes a fixed volume of cells and has marked squares, each corresponding to a volume of $0.1 \mu\text{l}$, thus allowing one to count the number of cells in a known volume. The number of cells in a square is counted; this is repeated for subsequent squares, until the total number of cells counted is at least 100, or until the cells in five squares have been counted. A volume of δ ml of cells is added to each well of the microtiter plate.

Let K denote the average number of cells counted per square (i.e., the number of cells counted divided by the number of squares considered). We estimate the average number of cells per well by $K \times \delta \times 2 \times 10^4$. (The 10^4 converts from cells per square to cells per ml; the 2 accounts for the fact that the cells were diluted in an equal volume of dye; δ is the volume of cells per well.)

8.2 Model for errors

We model the errors in each dilution/pipetting to have mean 0 and $\text{SD} \approx \epsilon \times$ (the target concentration of cells). Thus ϵ is the coefficient of variation for the cell concentration for the dilution (conditioning on the cell concentration in the sample from which the dilution was taken). Errors in the pipetting of cells into each of the wells are ignored.

Next, we model the cell counts for each square to be independent unbiased

Poisson counts. Finally, we assume that the dilution errors are stochastically independent, and that they are independent of the Poisson counts.

8.3 Error in the estimated number of cells per well

Let X denote the initial cell concentration, in cells per ml. 100 μ l of these cells are combined with 100 μ l of Trypan blue and placed in a hemacytometer; let X' denote the resulting cell concentration, in cells per square (i.e., cells per 10^{-4} ml). Let K denote the average number of cells counted in, say, m squares.

It is relatively easy to see that our estimate of the average number of cells per well is unbiased. We seek here to calculate $\mathbf{var}(20,000 \cdot K\delta)$.

Note that:

1. $\mathbf{E}X' = X/20,000$
2. $\mathbf{var}X' = (\epsilon\mathbf{E}X')^2 = (\epsilon X/20,000)^2$
3. $\mathbf{E}(K|X') = X'$
4. $\mathbf{var}(K|X') = X'/m$

Thus the variance of K is as follows:

$$\begin{aligned} \mathbf{var}(K) &= \mathbf{E}[\mathbf{var}(K|X')] + \mathbf{var}[\mathbf{E}(K|X')] \\ &= \mathbf{E}(X'/m) + \mathbf{var}(X') \\ &= X/(20,000m) + (\epsilon X/20,000)^2 \end{aligned}$$

The variance of our estimate, $20,000 \cdot K\delta$, is thus:

$$\begin{aligned}\mathbf{var}(20,000 \cdot K\delta) &= 20,000 \cdot X\delta^2/m + \epsilon^2\delta^2 X^2 \\ &= 20,000 \cdot \delta(\delta X)/m + \epsilon^2(\delta X)^2\end{aligned}$$

Note that δX is the true average number of cells per well.

8.4 Impact of cell count error on error in the frequency of responding cells

Let λ be the number of responding cells per well, let c be the number of cells per well (which had been written δX above), and let $\hat{\lambda}$ and \hat{c} denote the corresponding estimates. (Note that \hat{c} was written $20,000 \cdot \delta K$ above.)

We estimate the variance of $\hat{\lambda}$ by the SEM algorithm. We estimated the variance of \hat{c} above, as follows:

$$\mathbf{var}(\hat{c}) \approx 20,000 c\delta/m + \epsilon^2 c^2$$

where ϵ denotes the coefficient of variation for the volume delivered by the pipets (typically 0.01), δ denotes the volume of cells in each well in ml (typically 0.18), and m denotes the number of squares of cells counted (typically 5).

We seek the variance of $10^6 \hat{\lambda}/\hat{c}$. Note that by the delta method (i.e., Taylor expansion),

$$[\mathbf{CV}(\hat{\lambda}/\hat{c})]^2 \approx [\mathbf{CV}(\hat{\lambda})]^2 + [\mathbf{CV}(\hat{c})]^2$$

where $\mathbf{CV}(X)$ denotes the coefficient of variation of X ($\mathbf{SD}(X)/\mathbf{E}(X)$).

Thus, we obtain

$$\begin{aligned}
\mathbf{var}(10^6 \hat{\lambda}/\hat{c}) &\approx 10^{12}(\lambda/c)[\mathbf{var}(\hat{\lambda})/\lambda^2 + \mathbf{var}(\hat{c})/c^2] \\
&\approx 10^{12}\mathbf{var}(\hat{\lambda}) + 10^{12}\mathbf{var}(\hat{c})\lambda^2/c^4 \\
&\approx \frac{10^{12}\mathbf{var}(\hat{\lambda})}{c^2} + \frac{\delta 10^{12}\lambda^2 20,000}{mc^3} + \frac{\epsilon^2 10^{12}\lambda^2}{c^2}
\end{aligned}$$

Note that the first term gives the nominal variance (ignoring the cell count error), the second term gives the sampling error, and the third term gives the pipetting error.

Consider an example: let $\hat{\lambda} = 3.1$, $\mathbf{var}(\hat{\lambda}) = (0.3)^2 = 0.09$, $\hat{c} = 11,400$, $\epsilon = 1/100$, $m = 5$, and $\delta = 0.150$. Thus our estimated frequency of responding cells per 10^6 cells is 272. Our estimated variance is as follows:

$$\begin{aligned}
\mathbf{var}(10^6 \hat{\lambda}/\hat{c}) &\approx \frac{10^{12} \cdot 0.09}{(11,400)^2} + \frac{0.15 \cdot 10^{12} \cdot (3.1)^2 \cdot 20,000}{5 \cdot (11,400)^3} \\
&\quad + \frac{(0.01)^2 \cdot 10^{12} \cdot (3.1)^2}{(11,400)^2} \\
&= 693 + 3,892 + 7
\end{aligned}$$

In this example, the estimated SE of the frequency of responding cells per 10^6 cells is 26 when ignoring the cell count error, and 68 when considering the cell count error. The pipetting error is negligible.

TABLE LEGENDS

- Table 1.* Scintillation counts for the pair of plates from the first assay of subject #713 at density 11,400 cells/well.
- Table 2.* Maximum likelihood estimates and estimated standard deviations of model parameters for the results of the first assay of subject #713 at density 11,400 cells/well.
- Table 3.* Maximum likelihood estimates and estimated standard deviations of frequencies of responding cells per 10^6 cells for the results of the first assay of subject #713 at density 11,400 cells/well.
- Table 4.* Recentred maximized log-likelihoods for pairs of plates for different power transformations (Box–Cox analysis) for LDAs #713 and #711.
- Table 5.* Parameter estimates for plates from LDA #713 and LDA #711, analysed singly.
- Table 6.* Estimated frequencies per well for LDAs #713, #711 and NIH 1394.
- Table 7.* Estimated frequencies per 10^6 cells for LDAs #713, #711 and NIH 1394.
- Table 8.* Estimated plate parameters a , b and σ for the assays performed on subjects #713, #711 and NIH 1394.
- Table 9.* Counts per minute ($\times 10^{-2}$) read from Figure 2 of Langhorne and Fischer-Lindahl (1981).
- Table 10.* Maximum likelihood estimates of CTL-precursor frequencies and plate parameters at each density for the data in Table 9.
- Table 11.* Maximum likelihood estimates of responder frequencies and plate parameters for each experimental group for the data from S. Rodda.

Table 12. Maximum likelihood estimates of responder frequencies and plate parameters for the three LDAs from D. Koelle: DK2, KD and EL.

Table 13. Comparison of the cut-off method to our new method, for five cell densities from the Langhorne and Fischer-Lindahl data.

FIGURE LEGENDS

Figure 1. Mean scintillation counts in relation to cell density for the six-point LDA from #713.

Figure 2. Estimated number of responding cells vs. square root of scintillation count.

- a. #713: 11,400 cells/well, plate 1.
- b. #713: 1,990 cells/well, plate 2.
- c. #711: 155,200 cells/well, plate 1.
- d. #713: 25,067 cells/well, plate 2.

Figure 3. Normal quantile-quantile plots of residuals after fitting the model to power-transformed scintillation counts.

- a. $p = 1$ (untransformed).
- b. $p = 1/2$ (square root transformation).
- c. $p = 1/4$ (fourth-root transformation).
- d. $p = 0$ (natural log transformation).

Figure 4. Maximum likelihood estimates of frequencies ($\times 10^6$) of responding cells using two plates at each dilution: estimates plotted against #cells/well. Error bars correspond to $+/-$ one SD. Dotted line corresponds to estimated frequency of responding cells ($\times 10^6$) obtained using all the data.

- a. Subject #713 (one six-point LDA, one five-point LDA, plus single assays).
- b. Subject #711 (one five-point LDA, plus single assays).
- c. Subject NIH 1394 (one four-point LDA).

Figure 5. Maximum likelihood estimates of frequencies of CTL-Ps plotted

against number of responding cells.

Figure 6. Maximum likelihood estimates of frequencies of responders plotted against number of cells per well for the three LDAs from D. Koelle.

Table 1: Scintillation counts for the pair of plates from the first assay of subject #713 at density 11,400 cells/well.

	cells alone			gD2			gB2			Tetox		PHA
A	179	249	460	2133	2528	2700	2171	1663	6200	761	9864	12842
B	346	1540	306	8299	1886	3245	1699	2042	3374	183	7748	10331
C	117	249	1568	1174	4293	979	1222	1536	2406	6497	2492	6188
D	184	414	308	2801	2438	1776	2193	3211	1936	2492	5134	927
E	797	233	461	1076	1527	2866	2205	2278	2215	3725	3706	4050
F	305	348	480	3475	902	3654	2046	1285	1187	9899	5891	3646
G	1090	159	89	1472	90	3639	657	2393	1814	3330	4174	2389
H	280	571	329	4448	3643	881	3462	2118	1013	8793	4313	672
	1	2	3	4	5	6	7	8	9	10	11	12

A	178	111	630	4699	5546	5182	3982	3104	2496	4275	2831	9727
B	244	593	259	5622	560	1073	1479	2978	4362	5017	5074	10706
C	261	964	167	2991	3390	3986	2321	2157	3278	8216	3579	3538
D	221	544	299	1838	4368	322	1022	1554	2980	2732	6177	5212
E	533	228	615	1938	4046	333	3253	5091	2843	200	1110	5063
F	818	98	160	1032	3269	4918	1778	3810	2372	6355	1869	2695
G	234	472	243	4143	3351	1118	530	1174	1881	3447	4491	2945
H	169	481	478	3237	1565	2211	2460	2715	4793	3029	6225	4679
	1	2	3	4	5	6	7	8	9	10	11	12

Table 2: Maximum likelihood estimates and estimated standard deviations of model parameters for the results of the first assay of subject #713 at density 11,400 cells/well.

	λ_c	λ_d	λ_b	λ_t	a	b	σ
joint:							
plate 1	0.4 (0.1)	3.5 (0.3)	3.3 (0.3)	4.7 (0.3)	16.4 (0.9)	10.3 (0.3)	3.6 (0.5)
plate 2	0.4 (0.1)	3.5 (0.3)	3.3 (0.3)	4.7 (0.3)	14.8 (0.8)	9.4 (0.2)	2.9 (0.4)
separate:							
plate 1	0.3 (0.1)	3.0 (0.4)	2.8 (0.4)	4.4 (0.5)	16.7 (0.9)	10.3 (0.3)	3.5 (0.4)
plate 2	0.5 (0.1)	3.9 (0.4)	3.9 (0.4)	5.0 (0.5)	14.5 (0.7)	9.3 (0.2)	2.8 (0.3)

Table 3: Maximum likelihood estimates and estimated standard deviations of frequencies of responding cells per 10^6 cells for the results of the first assay of subject #713 at density 11,400 cells/well.

	f_d	f_b	f_t
joint	271 (67)	257 (64)	378 (92)
separate:			
plate 1	238 (60)	219 (56)	356 (87)
plate 2	306 (75)	299 (73)	400 (97)

Table 4: Recentred maximized log-likelihoods for pairs of plates for different power transformations (Box–Cox analysis) for LDAs #713 and #711.

(a)

#713		p			
cells/well	assay	1	0.5	0.25	0
31,333	2	0	-1	-6	-15
25,067	2	-5	0	-6	-21
18,800	2	-1	0	-5	-15
11,400	1	-6	0	-5	-20
9,000	2	-2	0	-2	-4
7,600	1	-13	0	-12	-24
5,700	1	-37	0	-3	-12
4,500	2	-21	0	-2	-8
3,800	1	-59	-4	0	-7
2,660	1	-86	-6	0	-4
1,990	1	-122	-24	-4	0
total		-353	-35	-44	-130

(b)

#711	p			
cells/well	1	0.5	0.25	0
155,200	-11	0	-37	-19
116,400	-20	-6	0	-31
80,000	-64	0	-12	-9
60,000	-56	-10	0	-13
40,800	-18	0	-5	-7
30,600	-1	0	-2	-7
total	-170	-16	-56	-87

Table 5: (a) Parameter estimates for plates from LDA #713, analysed singly.

#713							
# cells/well	λ_c	λ_d	λ_b	λ_t	a	b	σ
11,400	0.3	3.0	2.8	4.4	16.7	10.3	3.5
11,400	0.5	3.9	3.9	5.0	14.5	9.3	2.8
7,600	0.3	2.3	2.3	3.1	14.9	13.4	4.1
7,600	0.1	2.2	2.1	3.3	14.9	13.2	3.9
5,700	0.2	1.8	2.4	2.8	11.8	11.5	4.2
5,700	0.1	1.4	1.3	1.3	13.9	17.5	4.8
3,800	0.0	0.9	0.9	1.2	13.7	18.7	5.1
3,800	0.0	1.1	1.0	1.0	12.6	19.2	5.5
2,660	0.0	1.0	0.9	0.7	10.3	12.7	3.1
2,660	0.0	0.9	1.7	1.1	9.6	13.4	3.4
1,990	0.1	0.5	1.2	0.5	8.1	9.9	2.2
1,990	0.1	0.5	1.0	1.0	8.2	11.8	2.8
31,333	0.0	9.2	9.0	7.8	9.4	1.0	1.8
31,333	1.0	8.8	8.0	6.4	8.8	1.4	0.5
25,067	0.0	13.2	11.8	9.3	12.8	0.9	2.9
25,067	0.0	9.6	9.5	6.9	13.0	0.7	4.0
18,800	1.7	7.2	7.7	6.3	8.6	1.8	0.7
18,800	2.0	9.9	10.3	7.6	7.8	1.3	0.5
9,000	0.6	2.7	4.4	1.5	8.3	2.1	0.7
9,000	0.8	3.1	3.3	1.8	7.9	2.7	0.8
4,500	0.2	1.2	2.1	1.1	8.8	3.1	1.1
4,500	0.6	1.4	2.6	1.1	8.4	2.9	0.8

Table 5: (b) Parameter estimates for plates from LDA #711, analysed singly.

		#711						
#	cells/well	λ_c	λ_d	λ_b	λ_t	a	b	σ
	155,200	0.1	7.0	2.4	9.2	29.2	9.8	3.2
	155,200	0.0	6.7	2.7	8.7	29.0	10.6	3.3
	116,400	0.0	12.9	2.1	16.0	27.6	5.5	4.3
	116,400	0.0	5.9	1.0	7.5	28.2	11.2	3.3
	80,000	0.1	2.6	0.5	5.1	10.7	7.8	2.0
	80,000	0.2	2.0	0.3	5.8	10.5	6.1	1.5
	60,000	0.1	1.5	0.2	4.1	10.5	8.8	2.2
	60,000	0.2	2.2	0.2	3.9	10.4	7.7	1.9
	40,800	0.0	3.0	0.3	3.0	12.5	5.2	1.6
	40,800	0.1	2.5	0.4	3.5	12.7	5.5	2.0
	30,600	0.0	2.4	0.5	3.3	12.2	4.4	2.2
	30,600	0.0	1.5	0.2	1.8	11.4	6.2	1.9

Table 6: (a) Estimated frequencies per well for LDA #713.

# cells per well	#713								
	gD2			gB2			Tetox		
	λ	SD	CV	λ	SD	CV	λ	SD	CV
11,400	3.1	0.3	9	2.9	0.3	10	4.3	0.3	8
7,600	2.1	0.2	11	2.0	0.2	11	3.1	0.3	9
5,700	1.2	0.2	14	1.4	0.2	14	1.6	0.2	13
3,800	1.0	0.1	15	0.9	0.1	15	1.1	0.2	15
2,660	0.9	0.1	16	1.3	0.2	13	0.9	0.1	17
1,990	0.4	0.1	28	1.0	0.2	16	0.6	0.1	22
31,333	7.6	0.6	7	7.1	0.5	7	5.8	0.5	9
25,067	12.0	1.2	10	11.1	1.2	11	8.6	1.2	13
18,800	7.5	0.6	9	8.0	0.7	8	5.7	0.6	10
9,000	2.2	0.3	13	3.2	0.3	10	1.0	0.2	24
4,500	0.9	0.2	22	2.0	0.3	13	0.7	0.2	27
4,200	0.3	0.1	28	0.5	0.1	22	1.3	0.2	17
11,657	1.0	0.1	15	1.7	0.2	11	2.7	0.3	9
4,800	0.5	0.1	22	0.8	0.1	17	1.1	0.2	15
36,720	4.9	0.3	7	4.5	0.3	7	4.4	0.3	7
5,180	0.9	0.1	16	1.2	0.2	14	0.9	0.1	17
10,360	0.9	0.1	15	2.3	0.2	10	1.2	0.2	14
21,600	2.6	0.2	9	5.3	0.3	6	4.5	0.3	7
16,800	1.0	0.2	17	2.8	0.3	9	1.7	0.2	13
8,400	0.5	0.1	22	1.3	0.2	13	0.9	0.2	17

Table 6: (b) Estimated frequencies per well for LDA #711.

#711									
# cells per well	gD2			gB2			Tetox		
	λ	SD	CV	λ	SD	CV	λ	SD	CV
155,200	6.8	0.3	5	2.5	0.3	12	9.0	0.5	5
116,400	6.3	0.3	6	1.0	0.1	11	7.9	0.5	6
80,000	2.2	0.2	11	0.2	0.1	33	5.3	0.3	6
60,000	1.6	0.2	11	0.0	0.1	Inf	3.8	0.3	8
40,800	2.7	0.2	9	0.3	0.1	29	3.1	0.3	9
30,600	1.6	0.2	12	0.2	0.1	38	2.1	0.2	10
38,880	1.9	0.2	11	1.2	0.2	13	3.9	0.3	8
60,480	6.1	0.4	7	1.2	0.2	18	8.0	0.5	6
9,200	1.4	0.2	13	0.2	0.1	43	2.6	0.3	10
52,200	1.7	0.2	11	1.4	0.2	13	4.9	0.3	7
23,450	0.1	0.1	91	0.1	0.1	135	0.6	0.1	24
11,725	0.0	0.0	Inf	0.0	0.0	Inf	0.5	0.2	32

Table 6: (c) Estimated frequencies per well for LDA NIH 1394.

NIH 1394									
# cells per well	gD2			gB2			Tetox		
	λ	SD	CV	λ	SD	CV	λ	SD	CV
54,000	4.1	0.4	9	0.6	0.2	31	5.4	0.8	14
15,825	0.9	0.2	21	0.0	0.0	Inf	1.1	0.4	33
9,533	0.8	0.2	21	0.1	0.1	93	0.4	0.2	56
4,385	0.5	0.2	37	0.0	0.1	Inf	0.0	0.3	Inf

Table 7: Estimated frequencies per 10^6 cells for LDAs #713, #711 and NIH 1394. SD is the nominal estimated standard deviation. SD_a is the estimated standard deviation, adjusted for sampling error in the cell counts. CV_a is the adjusted coefficient of variation.

(a)

# cells per well	#713 gD2				#713 gB2				#713 Tetox			
	f	SD	SD_a	CV_a	f	SD	SD_a	CV_a	f	SD	SD_a	CV_a
11,400	271	25	67	25	257	25	64	25	378	30	92	24
7,600	272	30	69	25	268	30	68	25	404	37	100	25
5,700	217	31	59	27	239	33	64	27	272	36	72	26
3,800	268	39	73	27	247	38	68	28	289	42	79	27
2,660	341	55	96	28	477	64	127	27	324	56	93	29
1,990	209	58	75	36	516	81	142	28	317	71	100	32
31,333	241	18	24	10	227	17	23	10	186	16	20	11
25,067	479	48	58	12	443	49	57	13	343	46	52	15
18,800	399	34	43	11	424	35	45	11	303	30	36	12
9,000	246	31	48	20	351	36	63	18	109	26	31	28
4,500	203	45	54	27	445	58	88	20	166	44	51	31

(b)

# cells per well	#711 gD2				#711 gB2				#711 Tetox			
	f	SD	SD_a	CV_a	f	SD	SD_a	CV_a	f	SD	SD_a	CV_a
155,200	44	2	4	9	16	2	2	12	58	3	5	9
116,400	54	3	5	9	9	1	1	11	68	4	6	9
80,000	27	3	4	15	3	1	1	33	66	4	8	12
60,000	27	3	4	15	0	1	1	Inf	64	5	8	12
40,800	65	6	11	17	7	2	3	43	77	7	13	17
30,600	52	6	10	19	8	3	3	38	69	7	12	17

(c)

# cells per well	NIH 1394 gD2				NIH 1394 gB2				NIH 1394 Tetox			
	f	SD	SD_a	CV_a	f	SD	SD_a	CV_a	f	SD	SD_a	CV_a
54,000	77	7	10	13	11	3	4	32	99	14	14	17
15,825	54	11	12	23	0	3	3	Inf	71	23	24	34
9,533	88	18	20	22	8	7	7	94	41	23	24	57
4,385	123	46	47	38	0	30	30	Inf	0	58	58	Inf

Table 8: Estimated plate parameters a , b and σ for the assays performed on subjects #713, #711 and NIH 1394.

(a)

#713, assay 1			
cells/well	a	b	σ
11,400	16.4	10.3	3.6
11,400	14.8	9.4	2.9
7,600	15.2	13.4	4.2
7,600	14.9	13.2	3.9
5,700	13.7	15.0	5.3
5,700	13.9	17.3	4.8
3,800	13.7	18.4	5.0
3,800	12.6	19.2	5.5
2,660	10.3	12.6	3.1
2,660	9.5	13.5	3.4
1,990	8.0	9.9	2.2
1,990	8.3	11.8	2.8

(b)

#713, assay 2			
cells/well	a	b	σ
31,333	8.3	1.3	1.0
31,333	8.8	1.4	0.5
25,067	12.9	0.9	2.9
25,067	12.9	0.6	4.1
18,800	8.8	1.4	1.6
18,800	7.8	1.3	0.5
9,000	8.3	2.1	0.7
9,000	8.0	2.7	0.8
4,500	8.7	2.9	1.1
4,500	8.5	2.9	0.8

(c)

#711			
cells/well	a	b	σ
155,200	29.3	9.8	3.2
155,200	29.0	10.6	3.3
116,400	27.8	10.6	4.1
116,400	28.2	11.2	3.3
80,000	10.8	7.8	2.0
80,000	10.4	6.1	1.6
60,000	10.5	8.8	2.2
60,000	10.4	7.7	1.9
40,800	12.5	5.2	1.6
40,800	12.9	5.5	2.0
30,600	12.6	5.9	2.3
30,600	11.4	6.0	2.0

(d)

NIH 1394			
plate	a	b	σ
1	11.1	2.3	2.0
2	7.7	2.1	0.8
3	7.6	2.1	0.8
4	7.3	2.3	0.7
5	7.6	2.4	0.8

Table 9: Counts per minute ($\times 10^{-2}$) read from Figure 2 of Langhorne and Fischer-Lindahl (1981).

Cell density							
0	100	300	500	750	1000	3000	10000
5.2	4.8	5.4	5.8	6.0	6.0	8.4	9.0
5.2	5.0	5.4	6.0	6.0	6.4	9.2	9.4
5.4	5.0	5.6	6.0	6.2	6.6	9.4	9.4
5.4	5.4	5.6	6.0	6.6	7.2	10.8	11.8
5.6	5.4	5.6	6.2	6.8	8.4	11.0	11.8
5.6	5.4	5.8	6.2	6.8	8.6	11.2	12.0
5.6	5.6	5.8	6.4	7.0	9.2	12.2	12.0
5.8	5.6	5.8	6.4	7.6	9.2	12.2	12.0
5.8	5.6	6.0	6.4	8.0	9.4	12.2	12.2
5.8	5.6	6.0	6.8	8.2	9.4	12.4	12.2
5.8	5.6	6.2	7.4	8.4	9.8	12.6	12.4
6.0	5.8	6.2	7.4	8.4	10.2	12.6	12.4
6.0	5.8	6.2	8.2	8.8	11.0	13.0	12.6
6.0	5.8	6.4	8.2	9.4	11.2	13.2	13.0
6.0	5.8	6.4	8.6	9.8	11.6	13.6	13.6
6.0	5.8	6.4	9.2	10.0	11.6	13.6	13.6
6.0	5.8	8.2	10.2	10.2	11.8	13.8	13.6
6.2	6.0	8.4	10.4	11.2	11.8	14.4	14.0
6.2	6.0	8.6	11.0	11.8	12.4	14.8	14.2
6.2	6.2	8.8	11.2	12.4	12.6	15.2	14.4
6.4	6.4	8.8	11.8	13.2	13.4	15.4	14.4
6.4	6.4	9.0	12.4	13.6	14.6	15.6	14.6
6.4	6.8	10.2	12.6	13.8	15.2	16.0	14.6
6.4	9.6	14.4	12.8	15.2	16.4	16.6	15.6

Table 10: Maximum likelihood estimates of CTL-precursor frequencies and plate parameters at each density for the data in Table 9.

cell density	λ	a	b	σ
0	0.0 (0.0)	5.9 (0.1)	0.0 (0.0)	0.4 (0.1)
100	0.1 (0.1)	5.7 (0.1)	1.9 (0.2)	0.4 (0.1)
300	0.5 (0.1)	6.0 (0.1)	2.2 (0.1)	0.4 (0.1)
500	1.1 (0.2)	6.3 (0.2)	2.1 (0.1)	0.5 (0.1)
750	1.7 (0.3)	6.5 (0.1)	1.8 (0.1)	0.4 (0.1)
1,000	2.5 (0.3)	6.4 (0.3)	1.7 (0.1)	0.4 (0.1)
3,000	3.4 (0.4)	8.2 (0.2)	1.4 (0.1)	0.3 (0.1)
10,000	3.2 (0.4)	7.6 (0.5)	1.6 (0.2)	0.4 (0.1)

Table 11: Maximum likelihood estimates of responder frequencies and plate parameters for each experimental group for the data from S. Rodda.

group	λ_c	λ_t	λ_i	a	b	σ
post-immunization	0.0 (0.0)	0.4 (0.1)	1.3 (0.2)	14.3 (0.2)	6.9 (0.2)	1.8 (0.2)
				13.9 (0.2)	4.8 (0.3)	1.5 (0.1)
1:1 mixture	0.0 (0.0)	0.2 (0.1)	2.9 (0.2)	16.0 (0.3)	7.1 (0.2)	2.1 (0.2)
				16.1 (0.2)	6.0 (0.2)	1.6 (0.1)
preimmune	0.0 (0.0)	0.2 (0.1)	5.1 (0.3)	18.1 (0.4)	5.3 (0.2)	2.3 (0.3)
				19.1 (0.3)	8.2 (0.2)	2.5 (0.2)

Table 12: Maximum likelihood estimates of responder frequencies and plate parameters for each experimental group for the three LDAs from D. Koelle.

(a)

#cells/well	λ_0	λ_a
50,000	1.1 (0.3)	15.1 (1.0)
25,000	0.0 (0.0)	9.3 (0.7)
12,500	0.3 (0.2)	5.4 (0.5)
6,250	0.2 (0.1)	2.4 (0.4)
3,125	1.4 (1.1)	3.5 (2.4)
1,563	0.0 (0.0)	1.6 (1.3)
781	0.2 (0.6)	1.6 (1.2)

DK2

plates	a	b	σ
1,3	19.7 (0.6)	5.6 (0.2)	3.3 (0.4)
2,4	20.1 (0.7)	1.7 (1.0)	3.5 (0.4)

(b)

#cells/well	λ_0	λ_a
50,000	0.2 (0.1)	16.3 (0.9)
25,000	0.1 (0.1)	11.8 (0.7)
12,500	0.0 (0.0)	8.4 (0.6)
6,250	0.3 (0.1)	5.2 (0.5)
3,125	0.0 (0.0)	7.3 (1.6)
1,563	0.1 (0.2)	4.9 (1.1)
781	0.5 (0.3)	2.5 (0.7)

KD

plates	a	b	σ
1,3	17.9 (0.4)	7.7 (0.1)	2.8 (0.2)
2,4	21.1 (0.7)	4.8 (0.9)	4.2 (0.4)

(c)

#cells/well	λ_0	λ_a
50,000	0.3 (0.2)	14.5 (0.9)
25,000	0.0 (0.0)	8.9 (0.7)
12,500	0.1 (0.1)	5.3 (0.5)
6,250	0.0 (0.0)	2.1 (0.3)
3,125	0.4 (0.2)	2.3 (0.3)
1,563	0.5 (0.2)	1.7 (0.3)
781	0.8 (0.2)	0.8 (0.2)

EL

plates	a	b	σ
1,3	19.5 (0.5)	6.3 (0.2)	3.5 (0.3)
2,4	17.4 (0.4)	4.6 (0.3)	1.8 (0.2)

Table 13: Comparison of the cut-off method to our new method, for five cell densities from the Langhorne and Fischer-Lindahl data.

# cells	Cut-off method		New method		var(cut-off)/ var(new)
	λ	SD	λ	SD	
100	0.09	0.06	0.10	0.07	0.8
300	0.41	0.14	0.50	0.14	1.0
500	0.98	0.26	1.05	0.22	1.5
750	2.08	0.54	1.67	0.26	4.2
1000	2.48	0.68	2.52	0.33	4.2
joint	2029	303	1834	171	3.1

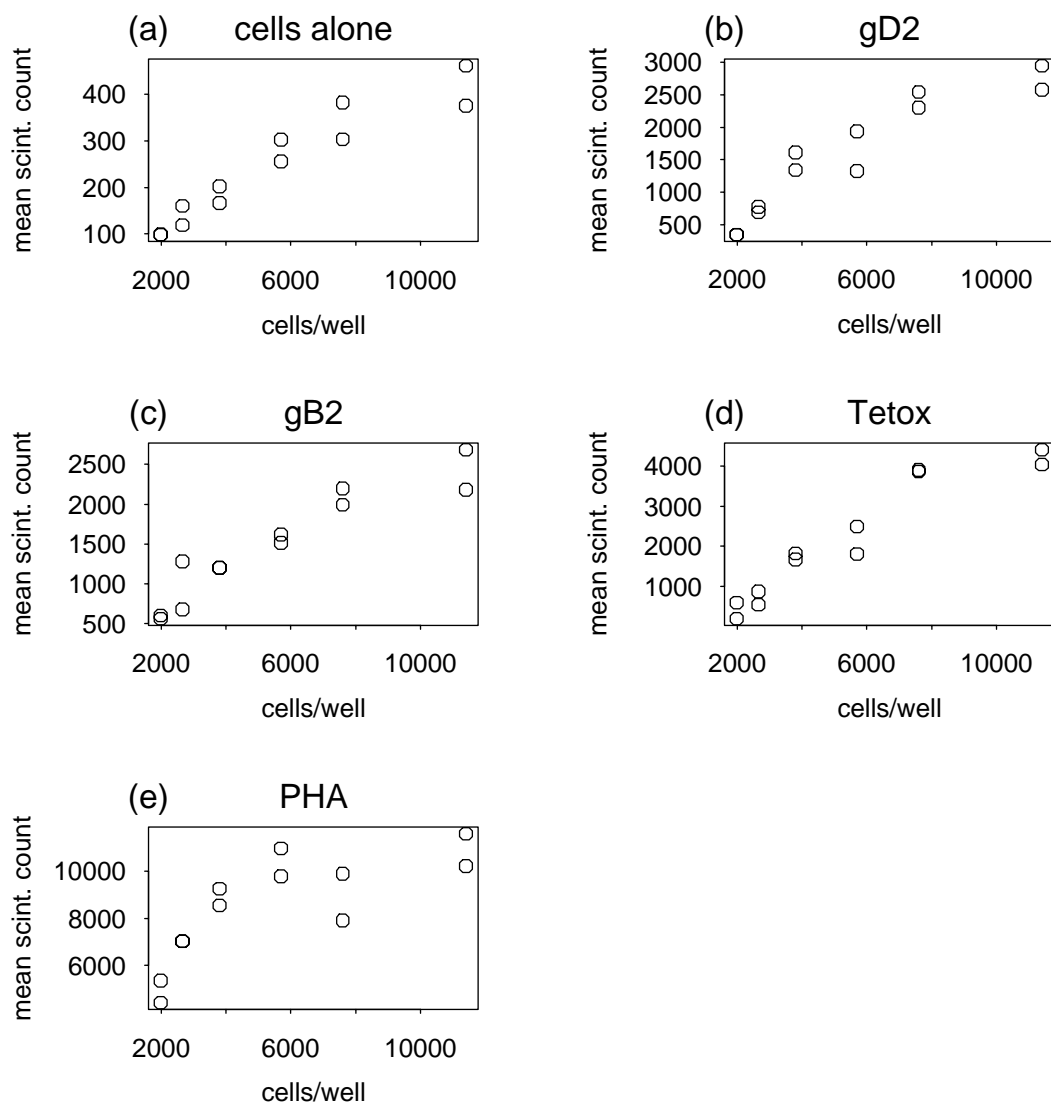


Figure 1: Mean scintillation counts in relation to cell density for the six-point LDA from #713.

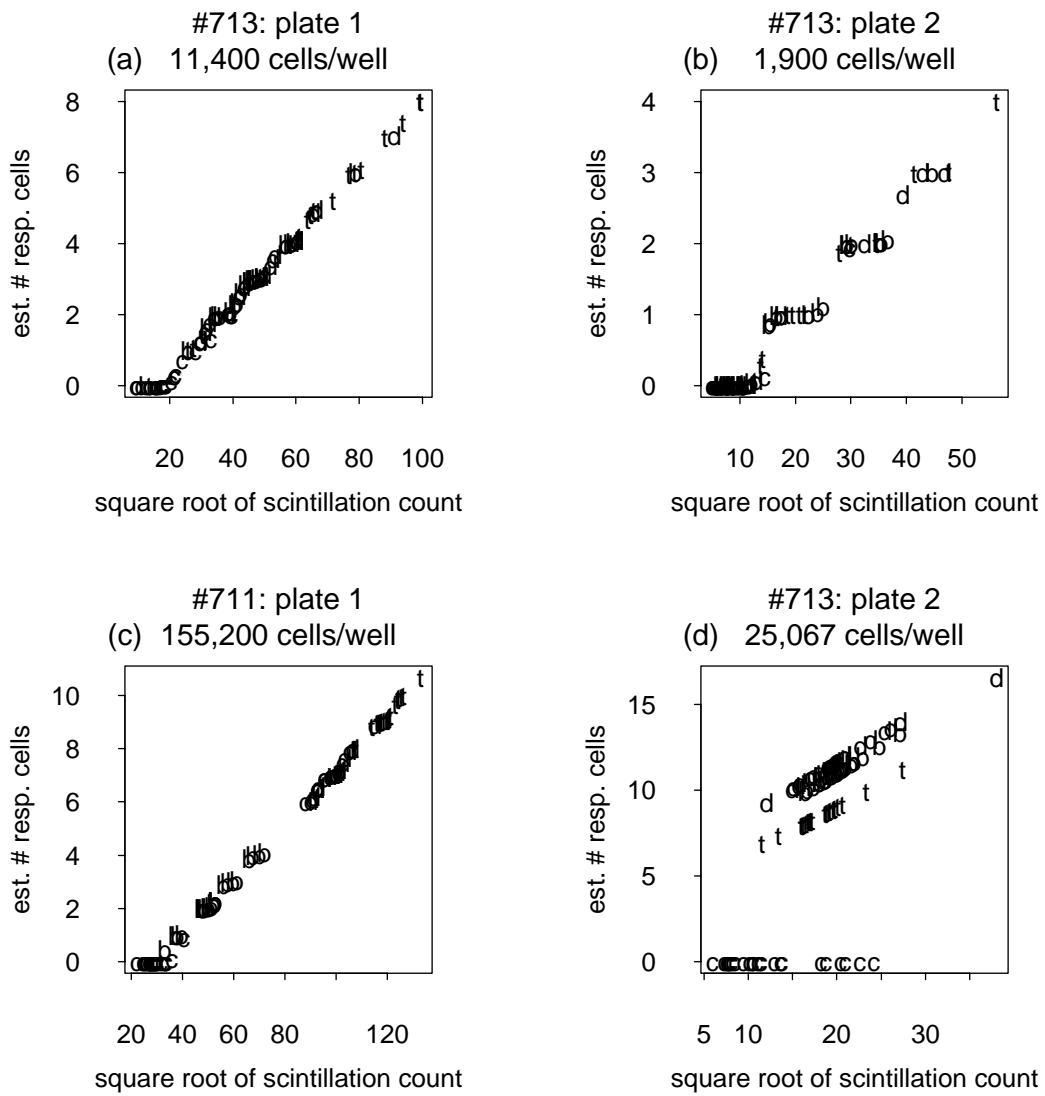


Figure 2: Estimated number of responding cells vs. square root of scintillation count.

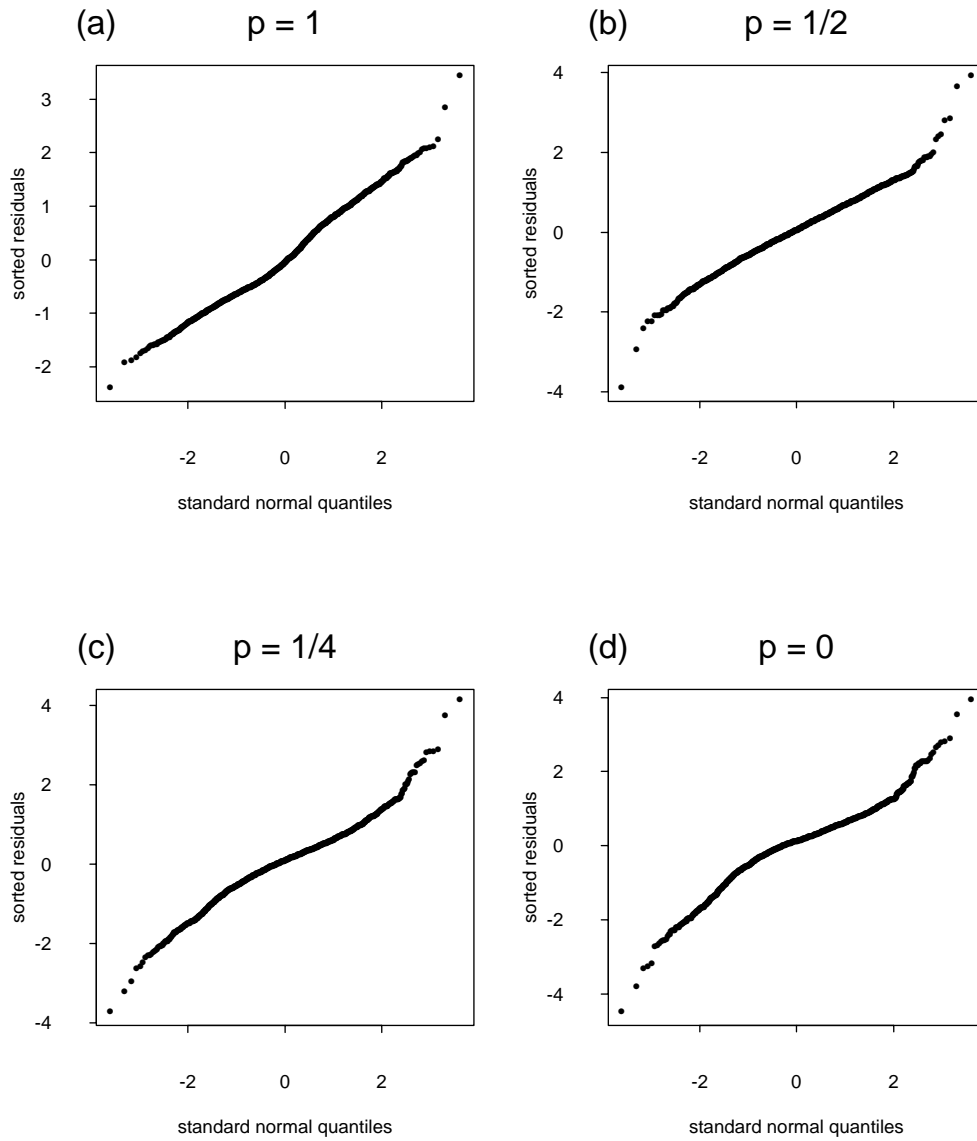


Figure 3: Normal quantile-quantile plots of residuals after fitting the model to power-transformed scintillation counts.

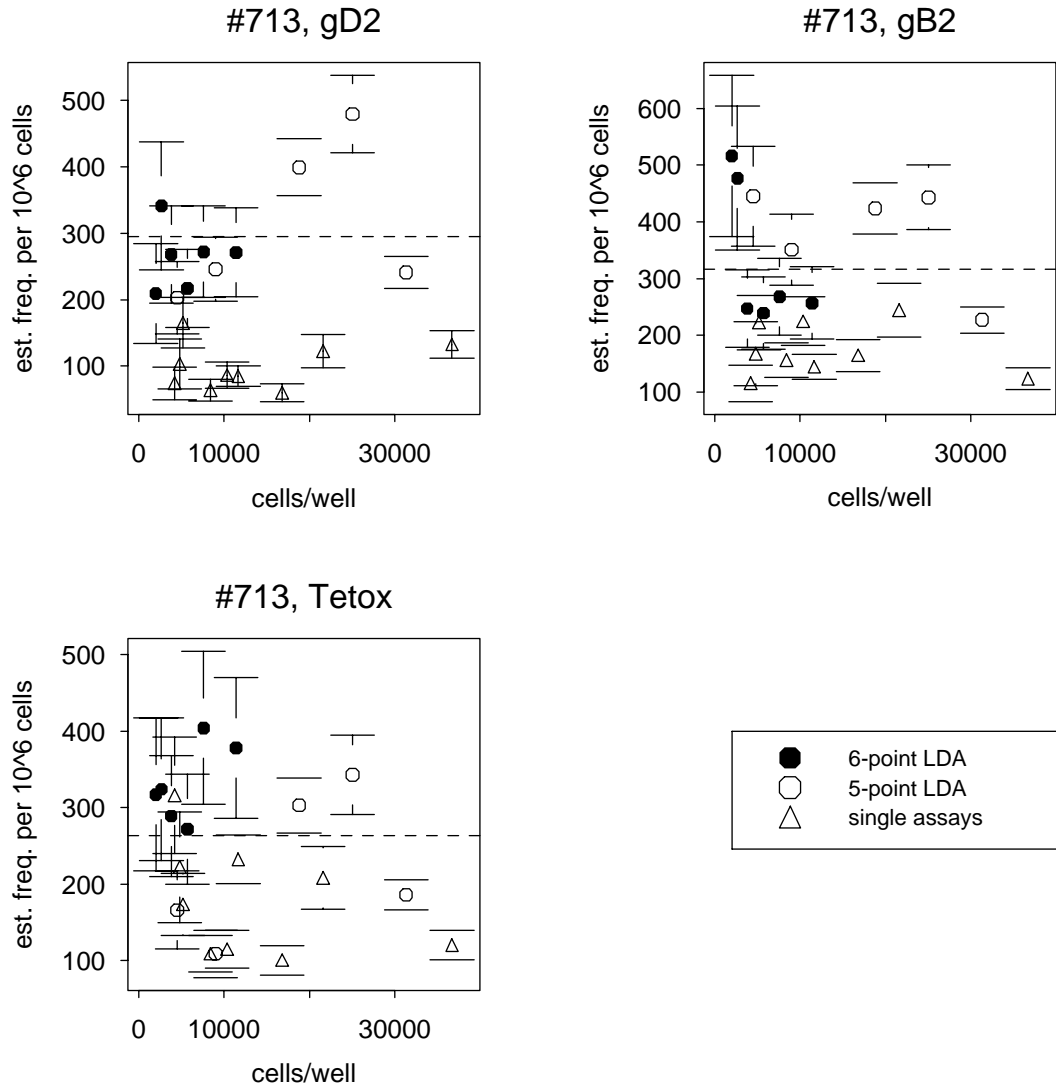


Figure 4: a: Subject #713 (one 6-point LDA, one 5-point LDA, and single assays). Maximum likelihood estimates of frequencies ($\times 10^6$) of responding cells using two plates at each dilution: estimates plotted against #cells/well. Error bars correspond to \pm one SD. Dotted line corresponds to estimated frequency of responding cells ($\times 10^6$) obtained using the two LDAs.

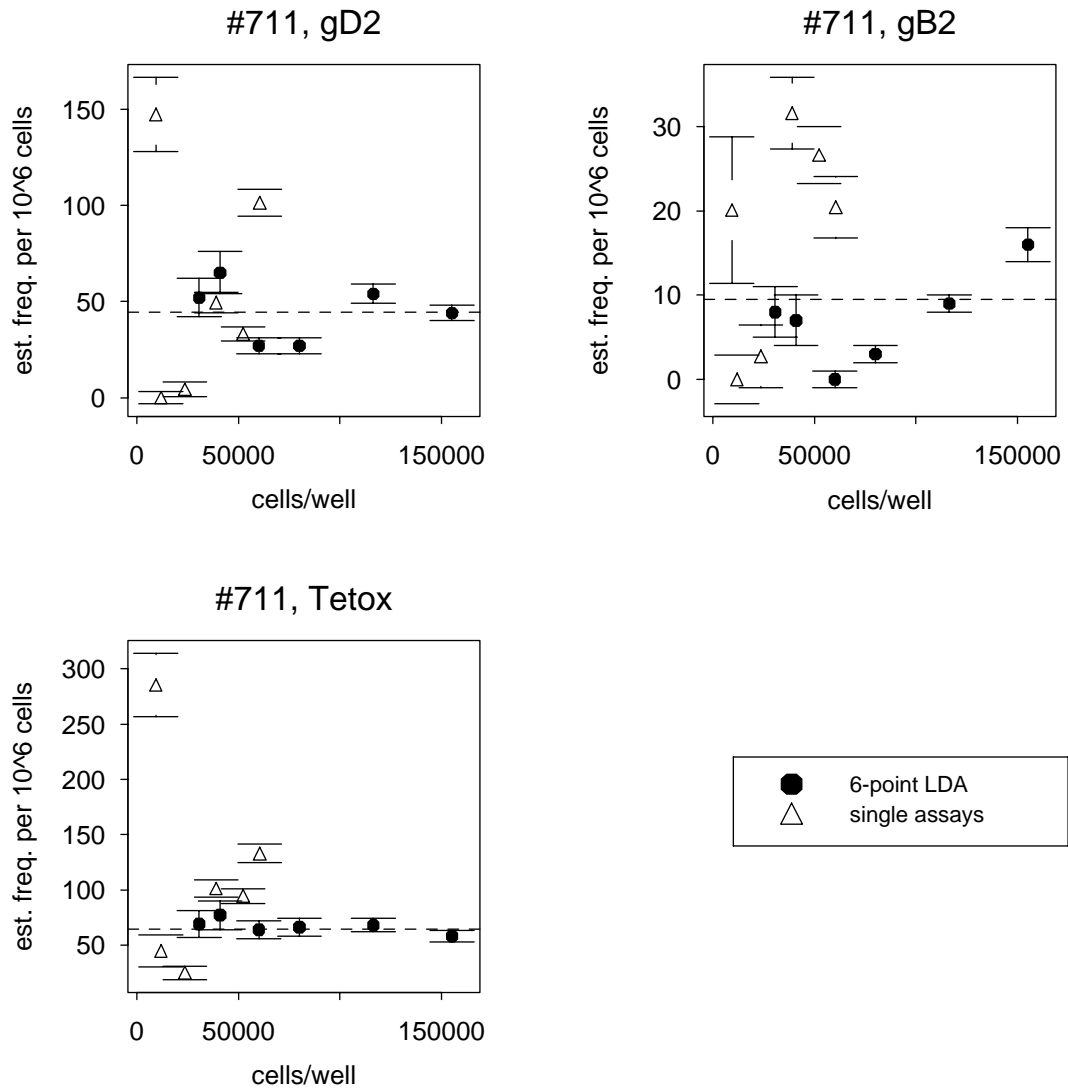


Figure 4: b: Subject #711 (one 6-point LDA and single assays). Maximum likelihood estimates of frequencies ($\times 10^6$) of responding cells using two plates at each dilution: estimates plotted against #cells/well. Error bars correspond to \pm one SD. Dotted line corresponds to estimated frequency of responding cells ($\times 10^6$) obtained using the data from the LDA.

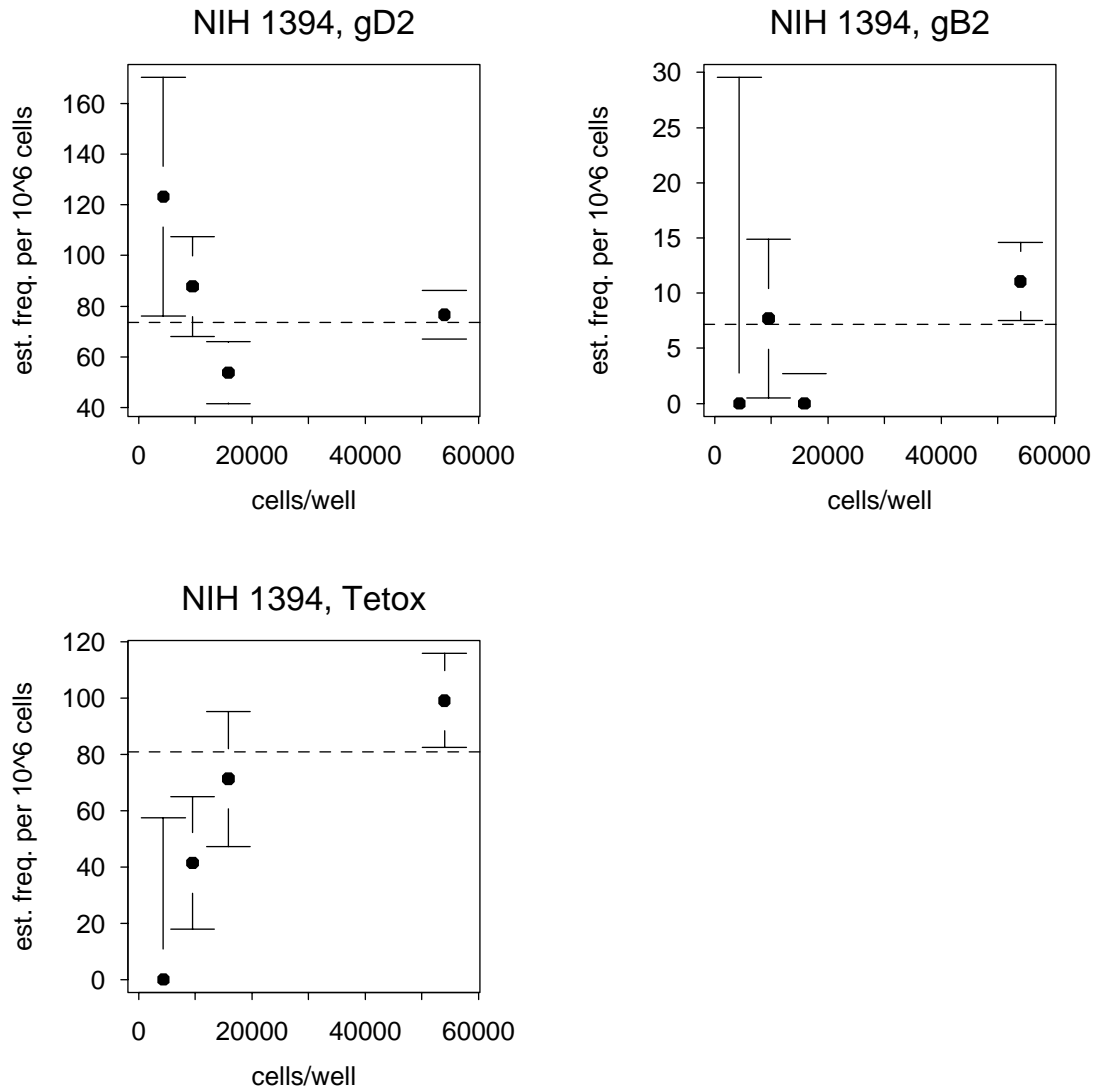


Figure 4: c: Subject NIH 1394 (one 4-point LDA). Maximum likelihood estimates of frequencies ($\times 10^6$) of responding cells using two plates at each dilution: estimates plotted against #cells/well. Error bars correspond to \pm one SD. Dotted line corresponds to estimated frequency of responding cells ($\times 10^6$) obtained using all the data.

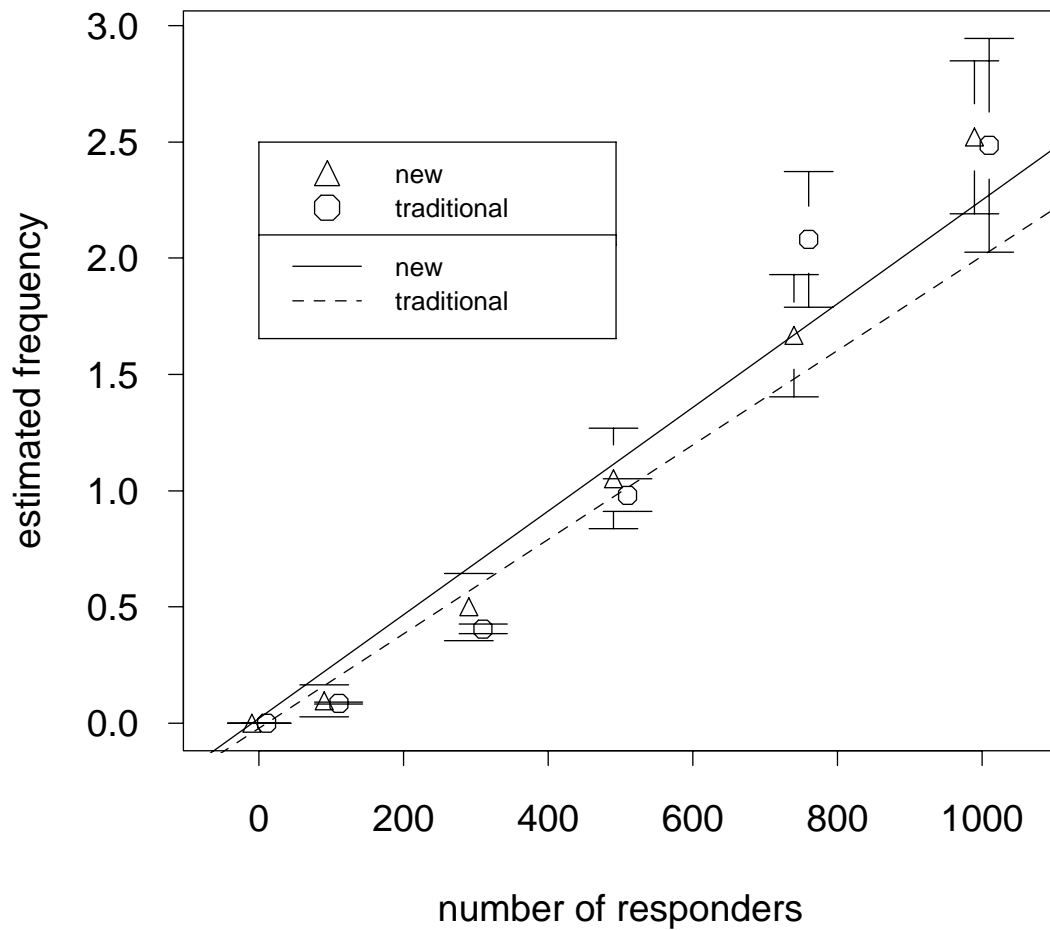


Figure 5: Maximum likelihood estimates of frequencies of CTL-Ps plotted against number of responding cells. The x-coordinates are offset slightly so that the points may be more easily distinguished.

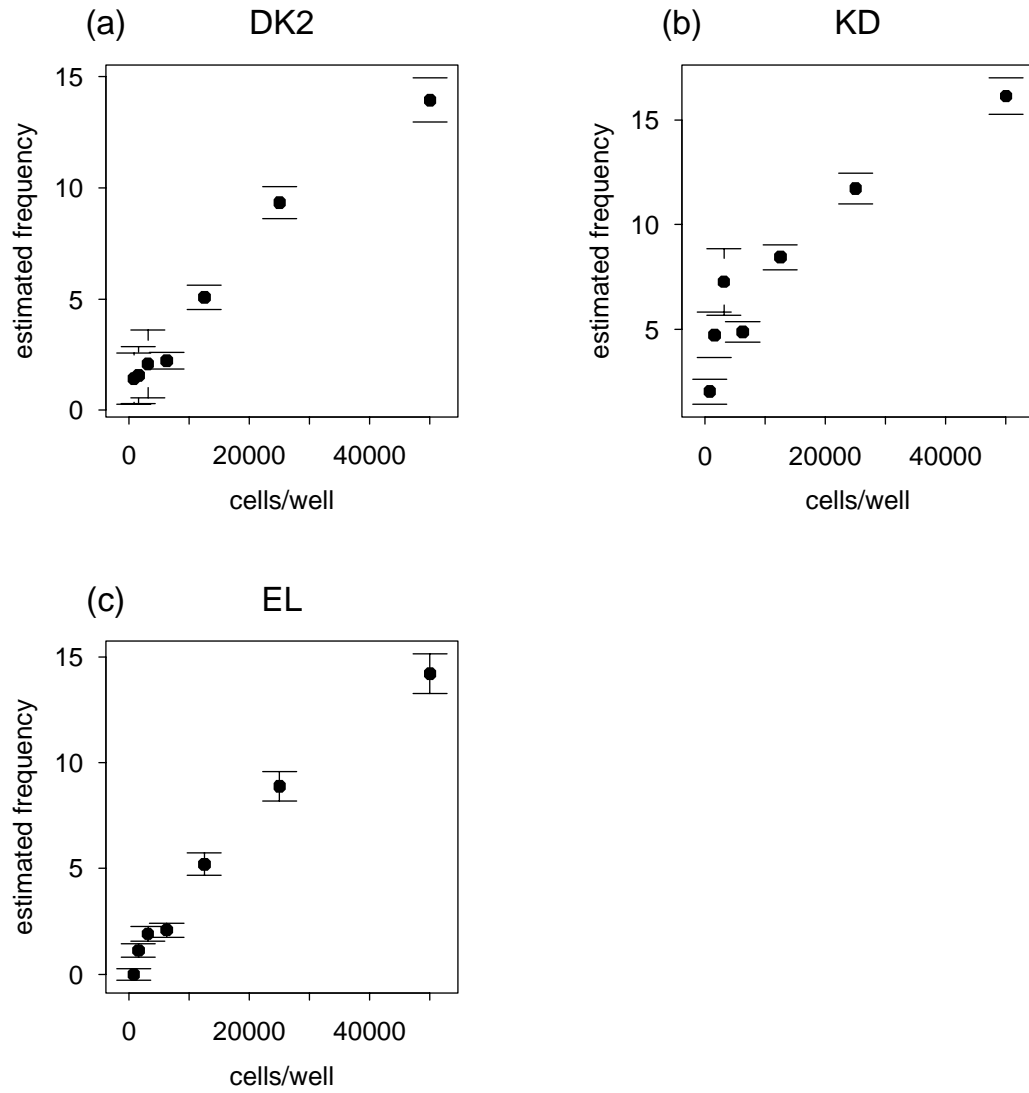


Figure 6: Maximum likelihood estimates of frequencies of responders plotted against number of cells per well for the three LDAs from D. Koelle.